Relevance of various Dirac covariants in hadronic Bethe-Salpeter wave functions in electromagnetic decays of ground state vector mesons

Shashank Bhatnagar,[1,*] Jorge Mahecha,[2,†] and Yikdem Mengesha[1]

[1]*Department of Physics, Addis Ababa University, P.O. Box 1176, Addis Ababa, Ethiopia*
[2]*Instituto de Física, Universidad de Antioquia UdeA; Calle 70 No. 52-21, Medellín, Colombia*

(Received 10 October 2013; revised manuscript received 5 June 2014; published 22 July 2014)

In this work we have employed the Bethe-Salpeter equation (BSE) under covariant instantaneous ansatz to study electromagnetic decays of ground state equal mass vector mesons ρ, ω, ϕ, ψ, and Y through the process $V \to \gamma \to e^+ + e^-$. We employ the generalized structure of the hadron-quark vertex function Γ that incorporates all Dirac structures from their complete set order by order in powers of the inverse of the meson mass. We have explicitly shown the derivation of this general form of this hadron-quark vertex function Γ (in terms of unknown coefficients) for a vector meson with the incorporation of all the Dirac structures (i.e., those dependent on external hadron momentum P, as well those dependent on internal hadron momentum q) as the solution of the full 4×4 Bethe-Salpeter equation. The unknown coefficients multiplying the various Dirac structures are calculated by reducing the 4×4 BSE to a determinantal form. These coefficients thus determined were also employed for the calculation of f_V values and gave good agreement with data, as well as an acceptable solution of the full BSE.

DOI: 10.1103/PhysRevD.90.014034 PACS numbers: 12.39.-x, 11.10.St, 12.40.Yx, 21.30.Fe

I. INTRODUCTION

Meson decays provide an important tool for exploring the structures of these simplest bound states in QCD and for studies on nonperturbative behavior of strong interactions. These studies have become a hot topic in recent years. Flavorless vector mesons play an important role in hadron physics due to their direct coupling to photons and thus provide an invaluable insight into the phenomenology of electromagnetic couplings to hadrons. Thus, a realistic description of vector mesons at the quark level of compositeness would be an important element in our understanding of hadron dynamics and reaction processes at scales where QCD degrees of freedom are relevant. There have been a number of studies [1–8] on processes involving strong, radiative, and leptonic decays of vector mesons. Such studies offer a direct probe of hadron structure and help in revealing some aspects of the underlying quark-gluon dynamics.

In this work we study electromagnetic decays of ground state equal mass vector mesons ρ, ω, ϕ, ψ, and Y (each comprising equal mass quarks) through the process $V \to \gamma^* \to e + e-$, which proceeds through the coupling of the quark-antiquark loop to the electromagnetic current in the framework of the Bethe-Salpeter equation (BSE), which is a conventional nonperturbative approach in dealing with relativistic bound state problems in QCD and is firmly established in the framework of field theory. From the solutions, we obtain useful information about the inner structure of hadrons, which is also crucial in high energy hadronic scattering and production processes. Despite the drawback of having to input a model dependent kernel, these studies have become an interesting topic in recent years since calculations have satisfactory results as more and more data are being accumulated. We get useful insight about the treatment of various processes using BSE due to the unambiguous definition of the four-dimensional (4D) BS wave function, which provides an exact effective coupling vertex (hadron-quark vertex) of the hadron with all its constituents (quarks).

We have employed the QCD motivated Bethe-Salpeter equation (BSE) under the covariant instantaneous ansatz (CIA) [9–14] to calculate this process. CIA is a Lorentz-invariant generalization of the instantaneous ansatz (IA). What distinguishes CIA from other three-dimensional (3D) reductions of BSE is its capacity for a two-way interconnection: an exact 3D BSE reduction for a $q\bar{q}$ system (for calculation of the mass spectrum), and an equally exact reconstruction of original 4D BSE (for calculation of transition amplitudes as 4D quark loop integrals). In these studies, the main ingredient is the 4D hadron-quark vertex function Γ, which plays the role of an exact effective coupling vertex of the hadron with all its constituents (quarks). The complete 4D BS wave function $\Psi(P, q)$ for a hadron of momentum P and internal momentum q comprises the two quark propagators (corresponding to two constituent quarks) bounding the hadron-quark vertex Γ. This 4D BS wave function is considered to sum up all the nonperturbative QCD effects in the hadron. Now one of the main ingredients in the 4D BS wave function (BSW) is its Dirac structure. The copious Dirac structure of BSW was already studied by Smith [15] much earlier. Recent studies

*Corresponding author.
shashank_bhatnagar@yahoo.com
†mahecha@fisica.udea.edu.co

[1,4,5] have revealed that various mesons have many different Dirac structures in their BS wave functions, whose inclusion is necessary to obtain quantitatively accurate observables. It was further noticed that all structures do not contribute equally for the calculation of various meson observables [1,7]. Further, it was amply noted in [16] that many hadronic processes are particularly sensitive to higher order Dirac structures in BS amplitudes. It was further noted in [16] that the inclusion of higher order Dirac structures is also important to obtain simultaneous agreement with experimental decay widths for a range of processes such as $V \to e^+e^-$, $V \to \gamma P$, $V \to PP$ for a given choice of parameters.

Toward this end, to ensure a systematic procedure of incorporating various Dirac covariants from their complete set in the BSWs of various hadrons (pseudoscalar, vector, etc.), we developed a naive power counting rule in Ref. [13], by which we incorporate various Dirac structures in BSW, order by order in powers of the inverse of the meson mass.

Using this power counting rule we calculated electromagnetic decay constants of vector mesons (ρ, ω, ϕ) using only the leading order (LO) Dirac structures [$i\gamma \cdot \varepsilon$ and $(\gamma \cdot \varepsilon)(\gamma \cdot P)/M$], where ε is the polarization vector of vector meson momentum P and mass M. However, in Ref. [14], we rigorously studied leptonic decays of unequal mass pseudoscalar mesons π, K, D, D_s, B and calculated the leptonic decay constants f_P for these mesons employing both the LO and the next-to-leading order (NLO) Dirac structures. The contributions of both LO and NLO Dirac structures to f_P was worked out. We further studied the relevance of both the LO and the NLO Dirac structures to this calculation.

In the present paper, we extended these studies to vector mesons and have employed both LO and NLO Dirac structures identified according to our power counting rule to calculate f_V for ground state vector mesons, $\rho, \omega, \phi, \psi, Y$, and in the process we studied the relevance of various Dirac structures to the calculation of decay constants f_V for vector mesons in the process $V \to e^+e^-$. Toward this end, we first explicitly show the derivation of the general form of the Hadron-quark vertex function Γ (in terms of unknown coefficients) for a vector meson with the incorporation of all the Dirac structures (i.e., those dependent on external hadron momentum P as well those dependent on internal hadron momentum q) as the solution of the full 4×4 Bethe-Salpeter equation. The unknown coefficients multiplying the various Dirac structures are calculated by reducing the BSE to a determinantal form. These coefficients thus calculated are also employed for the calculation of decay constants of vector mesons, which was found to give a good agreement with data, as well as an acceptable solution of the full BSE. We found that contributions from NLO Dirac structures are smaller than those of LO Dirac structures for all vector mesons. In what follows, we give a detailed discussion of the derivation of the full hadron-quark vertex function up to the NLO level in BSE under CIA and then the detailed calculation of decay constants f_V up to the NLO level after a brief review of our framework.

The paper is organized as follows: In Sec. II we discuss the structure of the BSW for vector mesons under CIA using the power counting rule we proposed earlier. We have also presented the derivation of the full 4×4 hadron-quark vertex function for a vector meson with the incorporation of all the Dirac covariants from BSE. In Sec. III we give the calculation of f_V for vector mesons. A detailed presentation of results and the numerical calculation is given in Sec. IV. Section V is relegated to discussion.

II. BSE UNDER CIA

We briefly outline the BSE framework under CIA. For simplicity, let us consider a $q\bar{q}$ system comprising scalar quarks with an effective kernel K, with the 4D wave function $\Phi(P, q)$, and with the 4D BSE,

$$i(2\pi)^4 \Delta_1 \Delta_2 \Phi(P, q) = \int d^4q K(q, q') \Phi(P, q'), \qquad (1)$$

where $\Delta_{1,2} = m_{1,2}^2 + p_{1,2}^2$ are the inverse propagators, and $m_{1,2}$ are (effective) constituent masses of quarks. The 4-momenta of the quark and antiquark, $p_{1,2}$, are related to the internal 4-momentum q_μ and total momentum P_μ of the hadron of mass M as $p_{1,2\mu} = \hat{m}_{1,2} P_\mu \pm q_\mu$, where $\hat{m}_{1,2} = [1 \pm (m_1^2 - m_2^2)/M^2]/2$ are the Wightman-Garding (WG) definitions of masses of individual quarks. Now it is convenient to express the internal momentum of the hadron q_μ as the sum of two parts, the transverse component, $\hat{q}_\mu = q_\mu - (q \cdot P) P_\mu / P^2$ that is orthogonal to total hadron momentum P_μ (i.e., $\hat{q} \cdot P = 0$ regardless of whether the individual quarks are on-shell or off-shell) and the longitudinal component $\sigma P_\mu = (q \cdot P) P_\mu / P^2$, which is parallel to P_μ. Thus we can decompose q_μ as $q_\mu = (\hat{q}, M\sigma)$, where the transverse component $\hat{q}$ is an effective 3D vector, while the longitudinal component $M\sigma$ plays the role of the fourth component and is like the time component. The 4D volume element in this decomposition is $d^4q = d^3\hat{q} M d\sigma$. To obtain the 3D BSE and the hadron-quark vertex, use an ansatz on the BS kernel K in Eq. (1), which is assumed to depend on the 3D variables $\hat{q}_\mu$, $\hat{q}'_\mu$ [12], i.e.,

$$K(q, q') = K(\hat{q}, \hat{q}'). \qquad (2)$$

Hence, the longitudinal component, σP_μ of q_μ, does not appear in the form $K(\hat{q}, \hat{q}')$ of the kernel. For reducing Eq. (1) to the 3D form of BSE, we define a 3D wave function, $\phi(\hat{q})$, as

$$\phi(\hat{q}) = \int_{-\infty}^{+\infty} M d\sigma \Phi(P, q). \qquad (3)$$

Dividing both sides of Eq. (1) by $\Delta_1\Delta_2$, then integrating both sides of Eq. (1) over $Md\sigma$, and making use of Eqs. (2) and (3), we obtain a covariant version of the Salpeter equation, which is in fact a 3D BSE,

$$(2\pi)^3 D(\hat{q})\phi(\hat{q}) = \int d^3\hat{q}' K(\hat{q},\hat{q}')\phi(\hat{q}'). \tag{4}$$

Here, $D(\hat{q})$ is the 3D denominator function defined as [13,14,17]

$$\frac{1}{D(\hat{q})} = \frac{1}{2\pi i}\int_{-\infty}^{+\infty}\frac{Md\sigma}{\Delta_1\Delta_2} = \frac{\frac{1}{2\omega_1}+\frac{1}{2\omega_2}}{(\omega_1+\omega_2)^2 - M^2},$$
$$\omega_{1,2}^2 = m_{1,2}^2 + \hat{q}^2, \tag{5}$$

whose value given above is obtained by evaluating the contour integration over inverse quark propagators in the complex σ plane by noting their corresponding pole positions (for details see [13,14]). This 3D BSE is used for making contact with mass spectra of $q\bar{q}$ mesons.

Further, making use of Eqs. (2) and (3) on the right-hand side (RHS) of Eq. (1), we get

$$i(2\pi)^4\Delta_1\Delta_2\Phi(P,q) = \int d^3\hat{q}' K(\hat{q},\hat{q}')\phi(\hat{q}'). \tag{6}$$

From the equality of the RHSs of Eqs. (4) and (6), we see that an exact interconnection between the 3D BS wave function $\phi(\hat{q})$ and the 4D BS wave function $\Phi(P,q)$ is thus brought out. We wish to mention that a similar covariant 3D reduction of the BSE with a (two way) connection between 3D and 4D wave functions similar to this approach was developed earlier by Sazdjian [18]. The 4D hadron-quark vertex function for scalar quarks under CIA can be identified as

$$\Delta_1\Delta_2\Phi(P,q) = \frac{D(\hat{q})\phi(\hat{q})}{2\pi i} \equiv \Gamma, \tag{7}$$

which can in turn be expressed as $\Phi(P,q) = \Delta_1^{-1}\Gamma\Delta_2^{-1}$, where $\Delta_{1,2}^{-1}$ are the scalar propagators of the two quarks flanking the hadron-quark vertex function, $\Gamma = D(\hat{q})\phi(\hat{q})/2\pi i$. It is to be noted that this hadron-quark vertex function satisfies a 4D BSE and thus can be profitably employed for the calculation of various transition amplitudes through various quark-loop diagrams.

Now, to adopt a fermionic system, we wish to mention that for a two-fermionic BSE, the BS amplitude has 16 components corresponding to the spinor indices of the two particles and transforms as the outer product of the two spinors. To formulate BSE for few-quark systems ($q\bar{q}$, qqq) within a common framework, it is more convenient to adopt the 16×1 column representation for a two-body ($q\bar{q}$ or qq) BS amplitude, instead of the more conventional 4×4 representation, though both are completely equivalent [15,19,20]. Thus the BSE in the 16×1 representation for the $q\bar{q}$ amplitude $\Psi(P,q)$ with a gluonic exchange interaction kernel (i.e., vector type) with a 3D support can be written as

$$i(2\pi)^4\Psi(P,q) = S_{F1}(p_1)S_{F2}(-p_2)\int d^4q' K(\hat{q},\hat{q}')\Psi(P,q');$$
$$K(\hat{q},\hat{q}') = F_{12} i\gamma_\mu^{(1)}\gamma_\mu^{(2)} V(\hat{q},\hat{q}'). \tag{8}$$

In the above equation, as stated above, K is one-gluon-exchange (o.g.e.) as regards color and spin dependence. Here F_{12} is the color factor, $(\lambda_1/2)\cdot(\lambda_2/2)$, and $(\gamma_\mu^{(1)}\gamma_\mu^{(2)})$ denotes the spin dependence, while the potential V involves the scalar structure of the gluon propagator in the perturbative (o.g.e.) as well as the nonperturbative (confinement) regimes. As regards the superscripts 1 and 2 on γ_μ, they indicate that the corresponding Dirac matrix gamma operates on particle 1 and particle 2, respectively. Thus, all $\gamma^{(1)}$'s commute with all $\gamma^{(2)}$'s. The spin dependent effects arise mainly due to the $\gamma_\mu^{(1)}\gamma_\mu^{(2)}$ dependence of the kernel for pairwise interactions. Here, $\gamma_\mu^{(1)}\gamma_\mu^{(2)} = \gamma^{(1)}\cdot\gamma^{(2)}$, and thus the interaction kernel has a $\boldsymbol{V}\cdot\boldsymbol{V}$ form and is a 4-scalar.

[Note that in the BSE corresponding to the 4×4 representation of $\Psi(P,q)$ (which is related to its 16×1 representation through standard transformations [15] of the charge conjugation of spinors), no indexing of γ_μ matrices is needed in either the two propagators or the kernel (see [20]). Thus on the left-hand side (LHS) of this equation, the inverse quark propagators (without the indices 1 or 2) should flank $\Psi(P,q)$, while on the RHS of this equation, the two γ_μ matrices coming from the kernel should be read with one on each side of $\Psi(P,q)$, but without the indices 1 or 2.]

The full structure of scalar function $V(\hat{q},\hat{q}')$ in the interaction kernel in Eq. (8), which is a sum of one-gluon exchange $V_{\rm OGE}$, and a confining term V_C is [9]

$$V(\hat{q}-\hat{q}') = V_{\rm OGE} + V_C,$$
$$V_{\rm OGE} = \frac{4\pi\alpha_S(Q^2)}{(\hat{q}-\hat{q}')^2},$$
$$V_C = \frac{3\omega_{q\bar{q}}^2}{4}\int d^3\boldsymbol{r} f(r) e^{i(\hat{q}-\hat{q}')\cdot\boldsymbol{r}},$$
$$f(r) = \frac{r^2}{(1+4a_0\hat{m}_1\hat{m}_2M^2r^2)^{1/2}} - \frac{C_0}{\omega_0^2}. \tag{9}$$

This confining term simulates an effect of an almost linear confinement ($\sim r$) for the heavy quark (c, b) sector, while retaining harmonic form ($\sim r^2$) for the light quark (u, d) sector as is believed to be true for QCD.

$$\omega^2_{q\bar{q}} = 4\hat{m}_1\hat{m}_2 M_> \omega_0^2 \alpha_S(M_>^2),$$
$$M_> = \mathrm{Max}(M, m_1 + m_2). \quad (10)$$

The values of basic constants are $C_0 = 0.29, \omega_0 = 0.158$ GeV, $\Lambda = 0.200$ GeV, $m_{u,d} = 0.265$ GeV, $m_s = 0.415$ GeV, $m_c = 1.530$ GeV, and $m_b = 4.900$ GeV [9,10,14]. However, the form of BSE in Eq. (8) is not convenient to use in practice since Dirac matrices lead to several coupled integral equations. However, a considerable simplification is effected by expressing them in Gordon-reduced form, which is permissible on the mass shells of quarks (i.e., on the surface $P \cdot q = 0$). Further for mass spectral calculations, what is important is to bring out the spin structure of the kernel. The Gordon reduced form of the fermionic BSE can be written as [9]

$$\Delta_1\Delta_2\Phi(P,q) = -i(2\pi)^{-4}\int d^4q' \tilde{K}_{12}(\hat{q},\hat{q}')\Phi(P,q'),$$
$$\tilde{K}_{12}(\hat{q},\hat{q}') = F_{12} V_\mu^{(1)} V_\mu^{(2)} V(\hat{q},\hat{q}'). \quad (11)$$

Here it is to be mentioned that $\pm V_\mu^{(1,2)}$ is obtained by multiplying $(m_{1,2} \mp i\gamma^{(1,2)}.p_{1,2})$ with $\gamma_\mu^{(1,2)}$. The structure of this Gordon reduced BSE in Eq. (11) is identical to the corresponding BSE for scalar quarks in Eq. (1), where the connection between $\Psi(P,q)$ in Eq. (8) and the auxiliary function $\Phi(P,q)$ is [9,10]

$$\Psi(P,q) = (m_1 - i\gamma^{(1)}\cdot p_1)(m_2 + i\gamma^{(2)}\cdot p_2)\Phi(P,q). \quad (12)$$

To simplify $V_\mu^{(1,2)}$ in the expression for pairwise interaction kernel $\tilde{K}_{12}$ entering in Eq. (11), we employ Gordon reduction on mass shells of individual quarks, which amounts to replacement [9,10]

$$V_\mu^{(1,2)} = \pm 2m_{1,2}\gamma_\mu^{1,2} = (p_{1,2} + p'_{1,2})_\mu + i\sigma_{\mu\nu}^{(1,2)}(p_{1,2} + p'_{1,2})_\nu. \quad (13)$$

Now to reduce the above BSE in Eq. (11) to the 3D form, all timelike components σ, σ' of momenta in $V_\mu^{(1)} V_\mu^{(2)}$ on the RHS of Eq. (9) are replaced by their on-shell values giving us the 3D form $\boldsymbol{V}_1 \cdot \boldsymbol{V}_2$. Thus

$$V_\mu^{(1)} V_\mu^{(2)} \Rightarrow \boldsymbol{V}_1 \cdot \boldsymbol{V}_2 = -4\hat{m}_1\hat{m}_2 M^2 - (\hat{q} - \hat{q}')^2 - 2(\hat{m}_1 - \hat{m}_2)P\cdot(\hat{q} + \hat{q}')$$
$$-i(2\hat{m}_1 P + \hat{q} + \hat{q}')_i \sigma_{ij}^{(2)}(\hat{q} - \hat{q}') + i(2\hat{m}_2 P - \hat{q} - \hat{q}')_i \sigma_{ij}^{(1)}(\hat{q} - \hat{q}')_j + \sigma_{ij}^{(1)}\sigma_{ij}^{(2)}. \quad (14)$$

The 3D form of BSE then works out as [10]

$$D(\hat{q})\phi(\hat{q}) = \omega^2_{q\bar{q}}\tilde{D}(\hat{q})\phi(\hat{q}),$$
$$\tilde{D}(\hat{q}) = 4\hat{m}_1\hat{m}_2 M^2(\nabla^2 + C_0/\omega_0^2) + 4\hat{q}^2\nabla^2 + 8\hat{q}\cdot\nabla + 18 - 8\boldsymbol{J}\cdot\boldsymbol{S} + \frac{4C_0}{\omega_0^2}\hat{q}^2. \quad (15)$$

This is reducible to the equation for a 3D harmonic oscillator with coefficients depending on the mass M and total quantum number N. The ground state wave functions [9,10,13] deducible from this equation have a Gaussian structure and are expressed as

$$\phi(\hat{q}) = e^{-\hat{q}^2/(2\beta^2)} \quad (16)$$

and is appropriate for making contact with a O(3)-like mass spectrum (for details see Ref. [9]). It is to be noted that this 3D BSE [in Eq. (15)], which is responsible for the determination of the mass spectra of mesons in CIA is formally equivalent (see [9,10,21]) to the corresponding mass spectral equation deduced earlier using the null-plane approximation (NPA) [22]. Thus the mass spectral predications for $q\bar{q}$ systems in BSE under CIA are identical to the corresponding mass spectral predictions for these systems in BSE under NPA [22] (see [9,10] for details).

We further wish to mention that a similar form for the ground state wave function in the harmonic oscillator basis using variational arguments has been used in [23]. In ground state wave function $\phi(\hat{q})$ in Eq. (16), β is the inverse range parameter that incorporates the content of BS dynamics and is dependent on the input kernel $K(q,q')$. The inverse range parameter β is determined by the criterion of minimizing the difference between the LHS and the RHS of the BSE. The values of β for different mesons are given in Table I.

A. Dirac structure of hadron-quark vertex function for vector mesons in BSE with power counting scheme

We now present the derivation of the hadron-quark vertex function for a vector meson. For transition amplitude calculations through quark-loop diagrams, what is important is to bring out the structure of the full 4D BS wave function $\Psi(P,q)$ in a 4×4 matrix form. The 4×4 version of $\Psi(P,q)$ in Eq. (12) can be written after taking account of standard transformations [15] of charge conjugation of spinors as [19]

$$\Psi(P,q) = (m_1 - i\gamma\cdot p_1)\Phi(P,q)(m_2 + i\gamma\cdot p_2), \quad (17)$$

where there is no indexing on gamma matrices and where the spin dependence of $\Phi(P,q)$ has now to be taken into account, and Φ should now be a 4×4 matrix in spinor space and should be expanded as a linear superposition of Dirac gamma matrices. In accordance with our power counting rule introduced in [13], we write the 4×4 form of $\Phi(P,q)$ as

$$\Phi(P,q) = [\Omega_V(P,q)]\Phi'(P,q), \tag{18}$$

where the entire spinor dependence is contained in $[\Omega_V(P,q)]$, while $\Phi'(P,q)$ is an auxiliary scalar function.

In our model, the relevant Dirac structures [15] in $\Phi(P,q)$ are incorporated in accordance with our recently proposed power counting rule [13,24], and the Dirac structure for a vector meson is expressed as [13]

$$\begin{aligned}[\Omega_V(P,q)] = {} & i(\gamma\cdot\varepsilon)A_0 + (\gamma\cdot\varepsilon)(\gamma\cdot P)\frac{A_1}{M} + [q\cdot\varepsilon - (\gamma\cdot\varepsilon)(\gamma\cdot q)]\frac{A_2}{M} \\ & + i\frac{A_3}{M^2}[(\gamma\cdot\varepsilon)(\gamma\cdot P)(\gamma\cdot q) - (\gamma\cdot\varepsilon)(\gamma\cdot q)(\gamma\cdot P) + 2(q\cdot\varepsilon)(\gamma\cdot P)] \\ & + (q\cdot\varepsilon)\frac{A_4}{M} + i(q\cdot\varepsilon)(\gamma\cdot P)\frac{A_5}{M^2} - i(q\cdot\varepsilon)(\gamma\cdot q)\frac{A_6}{M^2} + (q\cdot\varepsilon)[(\gamma\cdot P)(\gamma\cdot q) - (\gamma\cdot q)(\gamma\cdot P)]\frac{A_7}{M^3}. \end{aligned} \tag{19}$$

But since we take constituent quark masses, where the quark mass M is approximately half the hadron mass M, we can use the ansatz

$$q \ll P \sim M \tag{20}$$

in the rest frame of the hadron. Then each of the eight terms in the above equation receives suppression by different powers of $1/M$. Thus we can arrange these terms as an expansion in powers of $O(1/M)$. We can then see that in the expansion of $[\Omega_V]$ the structures associated with the coefficients A_0, A_1 have magnitudes $O(1/M^0)$ and are of LO. Those with A_2, A_3, A_4, A_5 are $O(1/M^1)$ and are NLO, while those with A_6, A_7 are $O(1/M^2)$ and are next to next leading order (NNLO). This naive power counting rule suggests that the maximum contribution to the calculation of any vector meson observable should come from Dirac structures $\gamma\cdot\varepsilon$ and $(\gamma\cdot\varepsilon)(\gamma\cdot P)/M$ associated with coefficients A_0 and A_1, respectively, followed by the higher order Dirac structures associated with the other four coefficients, A_2, A_3, A_4, A_5, and then by Dirac structures associated with coefficients A_6, A_7.

In this work we are interested in calculations up to next-to-leading orders. Thus we take the Dirac structure for a vector meson up to NLO terms as

$$\begin{aligned}[\Omega_V^{\mathrm{LO+NLO}}(P,q)] = {} & i(\gamma\cdot\varepsilon)A_0 + (\gamma\cdot\varepsilon)(\gamma\cdot P)\frac{A_1}{M} + [q\cdot\varepsilon - (\gamma\cdot\varepsilon)(\gamma\cdot q)]\frac{A_2}{M} \\ & + i[(\gamma\cdot\varepsilon)(\gamma\cdot P)(\gamma\cdot q) - (\gamma\cdot\varepsilon)(\gamma\cdot q)(\gamma\cdot P) + 2(q\cdot\varepsilon)(\gamma\cdot P)]\frac{A_3}{M^2} \\ & + (q\cdot\varepsilon)\frac{A_4}{M} + i(q\cdot\varepsilon)(\gamma\cdot P)\frac{A_5}{M^2}. \end{aligned} \tag{21}$$

which can be decomposed as $[\Omega_V^{\mathrm{LO+NLO}}(P,q)] = [\Omega_V^{\mathrm{LO}}(P)] + [\Omega_V^{\mathrm{NLO}}(P,q)]$, where $[\Omega_V^{\mathrm{LO}}]$ comprises only the leading order Dirac structures, comprising only the first two terms in the above expression (with coefficients A_0, A_1) that are functions of only the external momentum P, and are independent of the internal momentum q, while $[\Omega_V^{\mathrm{NLO}}(P,q)]$ comprises next-to-leading order Dirac structures, which are the remaining terms (with coefficients $A_2, \ldots, A_5$) and are dependent on both P and q. The choice of various Dirac covariants is constrained by required properties under charge conjugation and parity transformations [13,15,24], and where A_i are taken as the six dimensionless constant coefficients to be determined as acceptable solutions of BSE, while $\Phi'(P,q)$ is a scalar function.

Thus in 4×4 form, we can write Eq. (11) as

$$\begin{aligned} & i(2\pi)^4\Delta_1\Delta_2[\Omega_V^{\mathrm{LO}}(P) + \Omega_V^{\mathrm{NLO}}(P,q)]\Phi'(P,q) \\ & \quad = \int d^4q'\tilde{K}_{12}(\hat{q},\hat{q}')[\Omega_V^{\mathrm{LO}}(P) + \Omega_V^{\mathrm{NLO}}(P,q')]\Phi'(P,q'). \end{aligned} \tag{22}$$

In the above equation, it is to be noted that the right-hand side of the above equation can be split into two integrals. In the first integral, $[\Omega_V^{\mathrm{LO}}(P)]$ can be taken out of the integral sign, being independent of q', while in the second integral the integration is only performed over various terms of $[\Omega_V^{\mathrm{NLO}}(P,q')]$, which has to remain inside the integral with

various terms, all of which are functions of the integration variable q'.

Noting that the four-dimensional volume element, $d^4q' = d^3\hat{q}' M d\sigma'$, we integrate over the fourth component $M d\sigma'$ in both the integrals on the right-hand side of the above equation. Though integration over $M d\sigma'$ in the first integral is easy to perform, in the second integral we have both $[\Omega_V^{\rm NLO}]$ and Φ' under the integral sign, which are functions of integrating variable q', and hence are functions of $M d\sigma'$. Noting that $q' = \hat{q}' + \sigma' P$, we perform integration by parts over $M d\sigma'$. Performing integration over all the terms in the integrand of the second integral term by term, and making use of the orthogonality condition $P \cdot \varepsilon = 0$, and the obvious relation connecting the 3D and the 4D BS wave functions, $\phi'(\hat{q}') = \int M d\sigma' \Phi'(P, q')$, we obtain the equation

$$i(2\pi)^4 \Delta_1 \Delta_2 [\Omega_V^{\rm LO}(P) + \Omega_V^{\rm NLO}(P,q)]\Phi'(P,q) = \int d^3\hat{q}' \tilde{K}_{12}(\hat{q},\hat{q}')[\Omega_V^{\rm LO}(P) + \Omega_V^{\rm NLO}(P,\hat{q}')]\phi(\hat{q}'). \tag{23}$$

Dividing both sides of the above equation by $\Delta_1\Delta_2$, then integrating both sides over $M d\sigma$, and making use of Eq. (5) to carry out the contour integration on the right side, while again making use of integration by parts over $M d\sigma$ on the left side, and once again making use of the orthogonality condition $P \cdot \varepsilon = 0$, we get

$$(2\pi)^3 D(\hat{q})[\Omega_V^{\rm LO}(P) + \Omega_V^{\rm NLO}(P,\hat{q})]\phi'(\hat{q}) = \int d^3\hat{q}' \tilde{K}_{12}(\hat{q},\hat{q}')[\Omega_V^{\rm LO}(P) + \Omega_V^{\rm NLO}(P,\hat{q}')]\phi'(\hat{q}'). \tag{24}$$

It is to be noted that the right sides of Eqs. (23) and (24) are equal. This again leads to the two way interconnection between the 3D and the 4D BSE for the realistic case of a $q\bar{q}$ meson as well as the expression for the hadron-quark vertex function for the realistic case of a $q\bar{q}$ vector meson with all the Dirac covariants included from their complete set as

$$\Delta_1\Delta_2[\Omega_V^{\rm LO+NLO}(P,q)]\Phi'(P,q) = [\Omega_V^{\rm LO+NLO}(P,\hat{q})]\frac{D(\hat{q})\phi'(\hat{q})}{2\pi i} = \Gamma. \tag{25}$$

(In the above equation, it is to be noted that the LHS is a function entirely of q, while the RHS is a function entirely of $\hat{q}$.) This 4D hadron-quark vertex $\Gamma(\hat{q})$ as derived above satisfies a 4D BSE and provides a fully Lorentz-invariant basis for the evaluation of various transition amplitudes through various quark loop diagrams. As far as the expression for 3D BS wave function $\phi'(\hat{q})$ is concerned, as stated above, we notice that we can split the RHS of Eq. (24) into a sum of two integrals. Then, equating the terms multiplying $[\Omega_V^{\rm LO}(P)]$ on both sides of Eq. (24) (where $[\Omega_V^{\rm LO}(P)]$ is just a multiplying factor and can be canceled out), we get an equation that is exactly of the same form as the 3D version in Eq. (4). This justifies the solution $\phi'(\hat{q}) = \exp[-\hat{q}^2/(2\beta^2)]$, which is the same as $\phi(\hat{q})$ in Eq. (16). Thus from the above equation, we can write

$$\Phi(P,q) = \Delta_1^{-1}[\Omega_V^{\rm LO+NLO}(P,\hat{q})]\frac{D(\hat{q})\phi(\hat{q})}{2\pi i}\Delta_2^{-1}, \tag{26}$$

where it is to be noted that $\Phi(P,q) = [\Omega_V^{\rm LO+NLO}(P,q)]\Phi'(P,q)$. Putting $\Phi(P,q)$ above in Eq. (17) leads to the full reconstructed 4D BS wave function for the $q\bar{q}$ meson expressed as

$$\Psi(P,q) = S_F(p_1)\Gamma(\hat{q})S_F(-p_2) \tag{27}$$

and with the 4D normalized hadron-quark vertex function for a vector meson identified as

$$\Gamma(\hat{q}) = \frac{1}{2\pi i}[\Omega_V^{\rm LO+NLO}(P,\hat{q})]N_V D(\hat{q})\phi(\hat{q}) \tag{28}$$

and is a 4×4 matrix in spinor space, with $[\Omega_V^{\rm LO+NLO}(P,\hat{q})]$ containing the relevant Dirac structures.

The above expression can be expanded as

$$\begin{aligned}\Gamma(\hat{q}) = \Big\{ & i(\gamma\cdot\varepsilon)A_0 + (\gamma\cdot\varepsilon)(\gamma\cdot P)\frac{A_1}{M} \\ & + [\hat{q}\cdot\varepsilon - (\gamma\cdot\varepsilon)(\gamma\cdot\hat{q})]\frac{A_2}{M} \\ & + i[(\gamma\cdot\varepsilon)(\gamma\cdot P)(\gamma\cdot\hat{q}) - (\gamma\cdot\varepsilon)(\gamma\cdot\hat{q})(\gamma\cdot P) \\ & + 2(\hat{q}\cdot\varepsilon)(\gamma\cdot P)]\frac{A_3}{M^2} \\ & + (\hat{q}\cdot\varepsilon)\frac{A_4}{M} + i(\hat{q}\cdot\varepsilon)(\gamma\cdot P)\frac{A_5}{M^2}\Big\}\frac{1}{2\pi i}N_V D(\hat{q})\phi(\hat{q}),\end{aligned} \tag{29}$$

in which N_V is the 4D BS normalizer for the ground state vector meson with internal momenta q and is worked out in the framework of the CIA to give explicit covariance to the full fledged 4D BS wave functions, $\Psi(P,q)$, and hence to the hadron-quark vertex function, Γ, employed for the calculation of decay constants. In the structure of $\Gamma(\hat{q})$ above, $\phi(\hat{q})$ is the ground state 3D BS wave function for the vector meson with internal momenta q and is given in Eq. (16). This structure of the 4D hadron-quark vertex Γ in Eq. (29) incorporating all the Dirac covariants is thus derived from BSE.

Now, to calculate the parameters A_i (in the Dirac structure $[\Omega_V^{\rm LO+NLO}(P,\hat{q})]$ that enter into the BSE, Eq. (24), we first incorporate the kernel $\tilde{K}_{12}$ from

Eqs. (11) and (14) into Eq. (24) and perform integration over $d^3\hat{q}'$. After a sequence of steps, we arrive at the 3D equation

$$D(\hat{q})[\Omega_V^{\mathrm{LO+NLO}}(P,\hat{q})]\phi(\hat{q}) = \frac{3}{4}\omega_{q\bar{q}}^2\left[M^2\left(\nabla_{\hat{q}}^2 + \frac{C_0}{\omega_0^2}\right) + Q_q + 4 + 4\frac{C_0}{\omega_0^2}\hat{q}^2\right][\Omega_V^{\mathrm{LO+NLO}}(P,\hat{q})]\phi(\hat{q}). \tag{30}$$

Here, the operator $Q_q = 4\hat{q}^2\nabla_{\hat{q}}^2 + 8\hat{q}\cdot\nabla_{\hat{q}} + 6$. Now, it is to be noted here that the operators $\nabla_{\hat{q}}^2$ and Q_q operate on both $\phi(\hat{q})$ and $[\Omega_V^{\mathrm{LO+NLO}}(P,\hat{q})]$ on the RHS of the above equation. Here we have taken the eigenvalue equation for the operator Q_q as $Q_q\phi(\hat{q}) = -9\phi(\hat{q})$ [19] for ground state mesons studied here. Now, to eliminate the polarization vector ε from LHS and RHS in the above equation, we first multiply both sides of this by equation $(\gamma\cdot\varepsilon)$ from the left, and then we make use of the orthonormality relation for polarization vector $\varepsilon(P)$ for the V meson of 4-momentum P as

$$\varepsilon_\mu\varepsilon_\nu = \frac{1}{3}\left(\delta_{\mu\nu} + \frac{P_\mu P_\nu}{M^2}\right). \tag{31}$$

Further, making use of the orthogonality relations, $P\cdot\hat{q} = 0$ and $P\cdot\varepsilon = 0$, the BSE in Eq. (30) is reduced to the 4×4 form which is independent of ε as

$$\begin{aligned}
&D(\hat{q})\left[\left(iA_0 1 + \gamma\cdot P\frac{A_1}{M}\right) - \frac{2}{3}\gamma\cdot\hat{q}\frac{A_2}{M} + i\frac{4}{3}(\gamma\cdot P)(\gamma\cdot\hat{q})\frac{A_3}{M^2} + \left(\frac{\gamma.\hat{q}}{3}\frac{A_4}{M} + i\frac{\gamma\cdot\hat{q}\gamma\cdot P}{3}\frac{A_5}{M^2}\right)\right]\phi(\hat{q})\\
&= \frac{3}{4}\omega_{q\bar{q}}^2\left[\left(iA_0 1 + \gamma\cdot P\frac{A_1}{M}\right) - \frac{2}{3}\gamma\cdot\hat{q}\frac{A_2}{M} + i\frac{4}{3}(\gamma\cdot P)(\gamma\cdot\hat{q})\frac{A_3}{M^2} + \left(\frac{\gamma.\hat{q}}{3}\frac{A_4}{M} + i\frac{\gamma\cdot\hat{q}\gamma\cdot P}{3}\frac{A_5}{M^2}\right)\right]\\
&\quad\times\left[M^2\left(-\frac{1}{\beta^2} + \frac{\hat{q}^2}{\beta^4} + \frac{C_0}{\omega_0^2}\right) - 5 + 4\frac{C_0}{\omega_0^2}\hat{q}^2\right]\phi(\hat{q})\\
&\quad + \frac{3}{4}\omega_{q\bar{q}}^2[8]\left[-\frac{2}{3}\gamma\cdot\hat{q}\frac{A_2}{M} + i2(\gamma\cdot P)(\gamma\cdot\hat{q})\frac{A_3}{M^2} + \left(\frac{\gamma.\hat{q}}{3}\frac{A_4}{M} + i\frac{\gamma\cdot\hat{q}\gamma\cdot P}{3}\frac{A_5}{M^2}\right)\right]\phi(\hat{q}).
\end{aligned} \tag{32}$$

It is to be noted that if we carry out the trace operation over gamma matrices on both sides of the above equation, the BSE is reduced to the simple form

$$D(\hat{q})\phi(\hat{q}) = \frac{3}{4}\omega_{q\bar{q}}^2\left[M^2\left(-\frac{1}{\beta^2} + \frac{\hat{q}^2}{\beta^4} + \frac{C_0}{\omega_0^2}\right) - 5 + 4\frac{C_0}{\omega_0^2}\hat{q}^2\right]\phi(\hat{q}), \tag{33}$$

due to the orthogonality relation $\hat{q}\cdot P = 0$. This equation is independent of coefficients A_i's.

To work out the coefficients, A_i, we explicitly write the BSE in Eq. (32) as a 4×4 matrix equation for an on-shell hadron (with $-i\gamma\cdot P = M$). This 4×4 matrix equation is also expressible as a block diagonal 2×2 form in terms of the 2×2 unit matrix I, and Pauli spin matrices multiplying functions f_i of coefficients A_i. Taking $\hat{q}$ vector to point along any arbitrary spatial direction, we can express this 2×2 block diagonal form of Eq. (32) as

$$D(\hat{q})\begin{bmatrix} I(A_0+A_1)\phi(\hat{q}) & (\sigma\cdot\hat{q})f_1\phi(\hat{q}) \\ (\sigma\cdot\hat{q})f_2\phi(\hat{q}) & I(A_0+A_1)\phi(\hat{q})\end{bmatrix} = \frac{3}{4}\omega_{q\bar{q}}^2\begin{bmatrix} I(A_0+A_1)[X]\phi(\hat{q}) & (\sigma\cdot\hat{q})(f_1[X]+8f_3)\phi(\hat{q}) \\ (\sigma\cdot\hat{q})(f_2[X]+8f_4)\phi(\hat{q}) & I(A_0+A_1)[X]\phi(\hat{q})\end{bmatrix}, \tag{34}$$

where

$$[X] = \left[M^2\left(-\frac{1}{\beta^2}+\frac{\hat{q}^2}{\beta^4}+\frac{C_0}{\omega_0^2}\right)-5+4\frac{C_0}{\omega_0^2}\hat{q}^2\right],$$
$$f_1(A_i) = \frac{2A_2+4A_3-A_4+A_5}{3M},$$
$$f_2(A_i) = \frac{-2A_2-4A_3+A_4-A_5}{3M},$$
$$f_3(A_i) = \frac{2A_2+6A_3-A_4+A_5}{3M},$$
$$f_4(A_i) = \frac{-2A_2-6A_3+A_4-A_5}{3M}. \quad (35)$$

We now make use of the fact that if a matrix equation is expressed as LHS = RHS, then Det(LHS) = Det(RHS). Thus, if we take the determinant of both sides of this matrix equation and make use of the fact that $(\sigma\cdot\hat{q})^2=\hat{q}^2$, we get a single algebraic equation in coefficients A_i as

$$[D(\hat{q})]^2[(A_0+A_1)^2-\hat{q}^2 f_1(A_i)f_2(A_i)][\phi(\hat{q})]^2 = \left(\frac{3}{4}\omega_{q\bar{q}}^2\right)^2[(A_0+A_1)^2[X]^2-\hat{q}^2(f_1(A_i)[X] + 8f_3(A_i))(f_2(A_i)[X]+8f_4(A_i))][\phi(\hat{q})]^2. \quad (36)$$

However, if we do not take the determinant of both sides of Eq. (34), and instead, make use of equality $\mathrm{LHS}_{ij}=\mathrm{RHS}_{ij}$ in Eq. (34), we get four equations—discussion on this is relegated to the numerical section. We will now work out the coefficients A_i's using Eq. (36), so that they not only correspond to the solutions of the BSE, but also simultaneously lead to the calculation of decay constants of vector mesons, studied in the next section. In the process we will try to verify that the hadron-quark vertex function $\Gamma(\hat{q})$ (which involves $A_i s$), indeed corresponds to the solution of the BSE above. This study is relegated to the numerical section.

III. ELECTROMAGNETIC DECAYS OF VECTOR MESONS THROUGH THE PROCESS $V\to\gamma*\to e^+ + e^-$

A. Transition amplitude

The vector meson decay proceeds through the quark-loop diagram shown below (see Fig. 1).

The coupling of a vector meson of momentum P and polarization ε_μ to the photon is expressed via dimensionless coupling constant g_V, which can be described by the matrix element,

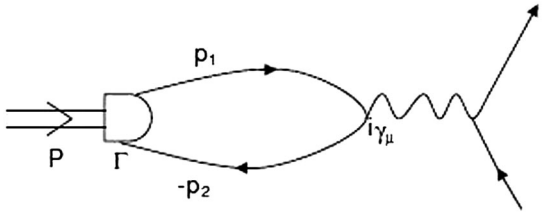

FIG. 1. Quark loop diagram for $V\to\gamma^*\to e^+ + e^-$ showing the coupling of electromagnetic current to the quark loop.

$$\frac{M^2}{g_V}\varepsilon_\mu(P) = \langle 0|\bar{Q}\hat{\Theta}\gamma_\mu Q|V(P)\rangle \quad (37)$$

(where Q is the flavor multiplet of the quark field and $\hat{\Theta}$ is the quark electromagnetic charge operator), which can in turn be expressed as a loop integral,

$$\frac{M^2}{g_V}\varepsilon_\mu(P) = \sqrt{3}e_Q\int d^4q\,\mathrm{Tr}[\Psi_V(P,q)i\gamma_\mu]. \quad (38)$$

Here e_Q arises from the flavor configuration of individual vector mesons and has values $e_Q = 1/\sqrt{2}, 1/3, 1/\sqrt{18}$, $2/3$, and $1/3$ for ρ,ϕ,ω,ψ, and Y, respectively, and the polarization vector ε_μ of the V meson satisfies $\varepsilon\cdot P=0$. Defining the leptonic decay constant f_V as $f_V = M/(e_Q g_V)$ [13], we can express

$$f_V\varepsilon_\mu(P) = \frac{\sqrt{3}}{M}\int d^4q\,\mathrm{Tr}[\Psi_V(P,q)i\gamma_\mu]. \quad (39)$$

Plugging the 4D BS wave function $\Psi_V(P,q)$ for a vector meson, which involves the 4D hadron-quark vertex function, Γ [in Eq. (29)] flanked by the Dirac propagators of the two quarks as in Eq. (27), into the above equation, evaluating the trace over the gamma matrices, and noting that only the components of terms on the right-hand side in the direction of ε_μ will contribute to the integral, we multiply both sides of the above integral by P_μ/M^2, and we can then express the leptonic decay constant f_V as

$$f_V = f_V^0 + f_V^1 + f_V^2 + f_V^3 + f_V^4 + f_V^5, \quad (40)$$

where $f_V^0, f_V^1, \ldots, f_V^5$ are contributions to f_V from the six Dirac structures associated with $A_0, A_1, \ldots, A_5$ in the expression for hadron-quark vertex function Γ and are expressed analytically in terms of $d\sigma$ integrations over the poles $\Delta_{1,2}$ of the quark propagators as

$$
\begin{aligned}
f_V^0 &= \sqrt{3}N_V\frac{A_0}{M}\int d^3\hat{q}D(\hat{q})\phi(\hat{q})\int\frac{Md\sigma}{2\pi i\Delta_1\Delta_2}4\left[\left(\frac{M^2}{6}+\frac{2}{3}m^2\right)+\frac{\Delta_1+\Delta_2}{6}\right],\\
f_V^1 &= \sqrt{3}N_V\frac{A_1}{M}\int d^3\hat{q}D(\hat{q})\phi(\hat{q})\int\frac{Md\sigma}{2\pi i\Delta_1\Delta_2}(-4mM),\\
f_V^2 &= \sqrt{3}N_V\frac{A_2}{M}\int d^3\hat{q}D(\hat{q})\phi(\hat{q})\int\frac{Md\sigma}{2\pi i\Delta_1\Delta_2}\left[-\frac{4}{3}m(\Delta_1-\Delta_2)\right],\\
f_V^3 &= \sqrt{3}N_V\frac{A_3}{M}\int d^3\hat{q}D(\hat{q})\phi(\hat{q})\int\frac{Md\sigma}{2\pi i\Delta_1\Delta_2}\left[-\frac{8}{3}(\Delta_1+\Delta_2)+\left(\frac{16}{3}m^2-\frac{4}{3}M^2\right)\right],\\
f_V^4 &= \sqrt{3}N_V\frac{A_4}{M}\int d^3\hat{q}D(\hat{q})\phi(\hat{q})\int\frac{Md\sigma}{2\pi i\Delta_1\Delta_2}\left[-\frac{2m}{3M}(\Delta_1+\Delta_2)+\left(\frac{4m^3}{3M}-\frac{1}{3}mM\right)\right],\\
f_V^5 &= \sqrt{3}N_V\frac{A_5}{M}\int d^3\hat{q}D(\hat{q})\phi(\hat{q})\int\frac{Md\sigma}{2\pi i\Delta_1\Delta_2}\left[\left(\frac{4}{3}m^2-\frac{2}{3}M^2\right)(\Delta_1-\Delta_2)\right].
\end{aligned}
\tag{41}
$$

In deriving the above expressions, we have made use of the relation showing the orthonormaity of the polarization vector, $\varepsilon(P)$ for the V meson of 4-momentum, P as in Eq. (31) to express the quantities involving dot products of ε with various momenta like $(p_1\cdot\varepsilon)(p_2\cdot\varepsilon)$, $(p_1\cdot\varepsilon)(q\cdot\varepsilon)$, and $(p_2\cdot\varepsilon)(q\cdot\varepsilon)$ (where it is to be noted that $\hat{q}\cdot\varepsilon = q\cdot\varepsilon$ on account of the orthogonality condition, $P\cdot\varepsilon = 0$) in terms of dot products of momenta as

$$
\begin{aligned}
(p_1\cdot\varepsilon)(p_2\cdot\varepsilon) &= \frac{1}{3}p_1\cdot p_2+\frac{(p_1\cdot P)(p_2\cdot P)}{3M^2},\\
(p_1\cdot\varepsilon)(q\cdot\varepsilon) &= \frac{1}{6}(p_1^2-p_1\cdot p_2)+\frac{(p_1\cdot P)(p_1\cdot P-p_2\cdot P)}{6M^2},\\
(p_2\cdot\varepsilon)(q\cdot\varepsilon) &= \frac{1}{6}(p_1\cdot p_2-p_2^2)+\frac{(p_2\cdot P)(p_1\cdot P-p_2\cdot P)}{6M^2}.
\end{aligned}
\tag{42}
$$

These dot products of momenta were in turn expressible in terms of the inverse propagators $\Delta_{1,2}$ as

$$
\begin{aligned}
p_1\cdot P &= \frac{1}{2}(\Delta_1-\Delta_2-M^2),\\
p_2\cdot P &= \frac{1}{2}(-\Delta_1+\Delta_2-M^2),\\
p_1\cdot p_2 &= m^2-\frac{1}{2}(\Delta_1+\Delta_2+M^2),\\
p_{1,2}^2 &= \Delta_{1,2}-m^2,\\
p_1\cdot q &= \frac{3}{4}\Delta_1+\frac{1}{4}(\Delta_2+M^2)-m^2,\\
p_2\cdot q &= -\frac{3}{4}\Delta_2-\frac{1}{4}(\Delta_1+M^2)+m^2,\\
P\cdot q &= \frac{1}{2}(\Delta_1-\Delta_2).
\end{aligned}
\tag{43}
$$

Thus all expressions for f_V^i above were expressible in terms of $\Delta_{1,2}$. Then carrying out integrations over the off-shell variable $d\sigma$ by the method of contour integrations by noting the pole positions in the complex σ plane,

$$
\begin{aligned}
&\Delta_1 = 0 \Rightarrow \sigma_1^{\pm} = \pm\frac{\omega_1}{M}-\hat{m}_1\mp i\epsilon,\\
&\Delta_2 = 0 \Rightarrow \sigma_2^{\mp} = \mp\frac{\omega_2}{M}-\hat{m}_2\pm i\epsilon,\\
&\omega_1^2 = \omega_2^2 = m^2+\hat{q}^2
\end{aligned}
\tag{44}
$$

(where $\hat{m}_1 = \hat{m}_2 = 1/2$ for equal mass quarks), we get the following integrals:

$$
\int\frac{Md\sigma}{\Delta_1\Delta_2}(\Delta_1+\Delta_2) = D_0(\hat{q});\qquad \int\frac{Md\sigma}{\Delta_1\Delta_2} = \frac{1}{D(\hat{q})},
\tag{45}
$$

where

$$
\begin{aligned}
D(\hat{q}) &= \omega D_0(\hat{q}),\\
D_0(\hat{q}) &= 4\omega^2-M^2.
\end{aligned}
\tag{46}
$$

Thus we can express the various components f_V^i $(i = 0,\ldots,5)$ of f_V in Eq. (41) as

$$
\begin{aligned}
f_V^0 &= \sqrt{3}N_V\frac{A_0}{M}\int d^3\hat{q}\phi(\hat{q})4\left[\frac{M^2}{6}+\frac{2}{3}m^2+\frac{D_0(\hat{q})}{6}\right],\\
f_V^1 &= \sqrt{3}N_V\frac{A_1}{M}\int d^3\hat{q}\phi(\hat{q})(-4mM),\\
f_V^2 &= 0,\\
f_V^3 &= \sqrt{3}N_V\frac{A_3}{M}\int d^3\hat{q}\phi(\hat{q})\left[-\frac{8}{3}D_0(\hat{q})+\frac{16}{3}m^2-\frac{4}{3}M^2\right],\\
f_V^4 &= \sqrt{3}N_V\frac{A_4}{M}\int d^3\hat{q}\phi(\hat{q})\left[-\frac{2m}{3M}D_0(\hat{q})+\frac{4m^3}{3M}-\frac{1}{3}mM\right],\\
f_V^5 &= 0.
\end{aligned}
\tag{47}
$$

Note that the components f_V^2 and f_V^5 are 0 on account of equal mass kinematics. Also note that each of the f_V^i involves the BS normalizer N_V. This is evaluated using the current conservation condition [13,14,17]

$$2iP_\mu = (2\pi)^4 \int d^4q \mathrm{Tr}\left\{ \bar{\Psi}(P,q)\left[\frac{\partial}{\partial P_\mu} S_F^{-1}(p_1)\right] \times \Psi(P,q) S_F^{-1}(-p_2)\right\} + (1 \rightleftharpoons 2). \quad (48)$$

Using Eqs. (17), (21), and (29) to write the BS wave function $\Psi_V(P,q)$ for a vector meson in the above equation, carrying out derivatives of inverse quark propagators of constituent quarks with respect to total hadron momentum P_μ, evaluating trace over products of gamma matrices, following the usual steps, and multiplying both sides of the equation by $P_\mu/(-M^2)$ to extract out the normalizer N_V from the above equation, we then express the above equation in terms of the integration variables $\hat{q}$ and σ. Noting that the 4D volume element $d^4q = d^3\hat{q}Md\sigma$, we then perform the contour integration in the complex σ plane by making use of the corresponding pole positions. For details of these mathematical steps involved in the calculations of BS normalizers for vector and pseudoscalar mesons see [13,14], where in the present calculation, we take both the LO and the NLO Dirac structures for vector mesons in their respective 4D BS wave functions $\Psi_V(P,q)$. Then integration over the variable $\hat{q}$ is finally performed to extract out the numerical results for N_V for different vector mesons. The calculation of N_V is quite complex due to the six Dirac structures involved in the calculation. The structure of the BS normalizer is of the form

$$N_V^{-2} = i(2\pi)^2 \int d^3\hat{q} D^2(\hat{q}) \phi^2(\hat{q}) \sum_{ij} A_i A_j I_{ij}(m, M, \hat{q}, S). \quad (49)$$

Here, $A = (A_0, A_1, A_2, A_3, A_4, A_5)$. The N_V depend on parameters A_i and $I_{ij}(m, M, \hat{q}, S)$. The $I_{ij}(m, M, \hat{q}, S)$ are extremely involved functions of $m, M, \hat{q}$, and S, where the elements S_i, $i = (1, \ldots, 6)$ are analytic results of contour integrations over the off-shell parameter $d\sigma$ in the complex σ plane. Explicit expressions of S and I_{ij} are listed at the end of the manuscript in the Appendix.

The final expression for the BS normalizer has the form

$$\begin{aligned} N_V^{-2} = \frac{\pi^{5/2}}{72M^7\beta^3} e^{m^2/(2\beta^2)} \Bigg\{ & [G_{13}(m,M,A) + G_{11}(m,M,A)\beta^2 + G_9(m,M,A)\beta^4] K_0\left(\frac{m^2}{2\beta^2}\right) \\ & + [G_{13}(m,M,A) + G_{11}(m,M,A)\beta^2 + G_9(m,M,A)\beta^4 + G_7(m,M,A)\beta^6] K_1\left(\frac{m^2}{2\beta^2}\right) \\ & + \Bigg[H_5(m,M)\beta^6 U\left(\frac{1}{2}, -3, \frac{m^2}{\beta^2}\right) \\ & + H_7(m,M)\beta^4 U\left(\frac{1}{2}, -2, \frac{m^2}{\beta^2}\right) \\ & + H_{11}(m,M) U\left(\frac{1}{2}, 0, \frac{m^2}{\beta^2}\right)\Bigg] \beta^2 A_3 A_5 \Bigg\}. \end{aligned} \quad (50)$$

Here, $K_n(x)$ is the second class modified Bessel function, $U(a,b,x)$ is the confluent hypergeometric function, G_n and H_n are polynomials of the nth degree in m and M, and the G_n are quadratic functions of the A_i coefficients.

In these expressions, $\phi(\hat{q})$ is a decaying function of $\hat{q}^2$. Thus despite the fact that the integrands contain growing factors like $\hat{q}^2$, the overall integrals converge and can be analytically integrated. Then, the f_V^i $(i = 0, \ldots, 5)$ can be expressed in the following analytic form:

$$\begin{aligned} f_V^0 &= \frac{A_0}{M} N_V 16\sqrt{\frac{2}{3}}\pi^{3/4}\beta^{3/2}(2m^2 + 3\beta^2), \\ f_V^1 &= -A_1 N_V 8\sqrt{6}\pi^{3/4}\beta^{3/2} m, \\ f_V^2 &= 0, \\ f_V^3 &= \frac{A_3}{M^2} N_V \frac{2\pi^{1/4}}{\sqrt{3}}\sqrt{\beta}\Bigg\{ 3M\sqrt{2\pi}\beta(-4m^2 + M^2 - 28\beta^2) \\ &\quad + 2e^{m^2/(4\beta^2)} m^2 \left[2m^2 K_0\left(\frac{m^2}{4\beta^2}\right) + (2m^2 - M^2 + 16\beta^2) K_1\left(\frac{m^2}{4\beta^2}\right)\right]\Bigg\}, \\ f_V^4 &= -\frac{A_4}{M^3} N_V \frac{4\pi^{1/4}}{\sqrt{3}}\sqrt{\beta}\Bigg\{ m^2 M^2 e^{m^2/(4\beta^2)} K_1\left(\frac{m^2}{4\beta^2}\right) + 2\sqrt{\pi}\beta^3 \left[3\sqrt{2}M - 8\beta U\left(-\frac{3}{2}, -2, \frac{m^2}{2\beta^2}\right)\right]\Bigg\}, \\ f_V^5 &= 0, \end{aligned} \quad (51)$$

TABLE I. Decay constant $f_V^{\mathrm{TH.}}$ values (in GeV) for ρ, ω, ϕ, ψ, and Y mesons in BSE-CIA with the individual contributions f_V^0, f_V^1, f_V^2, f_V^3, f_V^4, f_V^5 from various Dirac covariants along with the contributions from LO and NLO covariants and also their % contributions for the parameter set: $A_0 = 1$, $A_1 = 0.0064$, $A_2 = 0.0048$, $A_3 = -0.453$, $A_4 = -0.79$, $A_5 = -2.08474$ (with average error with respect to the experimental data of 3.58%).

	β	f_V^0	f_V^1	f_V^3	f_V^4	f_V^{LO}	f_V^{NLO}	$f_V^{\mathrm{LO}}(\%)$	$f_V^{\mathrm{NLO}}(\%)$	$f_V^{\mathrm{TH.}}$	f_V^{EXP}
$\rho(770)$	0.246	0.1014	−0.0006	0.0782	0.01298	0.1008	0.0912	53%	47%	0.192	0.220
$\omega(782)$	0.249	0.1025	−0.0006	0.0790	0.0129	0.1019	0.0919	53%	47%	0.194	0.195
$\phi(1020)$	0.294	0.1261	−0.0008	0.0787	0.0154	0.1253	0.0941	57%	33%	0.220	0.228
$\psi(1S)$	0.612	0.2884	−0.00225	0.0989	0.0214	0.286	0.1203	71%	29%	0.406	0.410
$Y(1S)$	1.33	0.559	−0.004	0.125	0.0293	0.555	0.1543	79%	21%	0.7097	0.708

with N_V given in the previous equation.

IV. RESULTS

A. Numerical calculation

Equation (51), which expresses decay constants f_V^i of vector mesons in terms of the parameters $A \equiv (A_0, A_1, A_2, A_3, A_4, A_5)$, is a nonlinear function of the A_i's. It is to be noted that these parameters A_i are contained in the expression for the hadron-quark vertex Γ in Eq. (29), which originates as a solution of 4D BSE. There are two ways to numerically choose those parameters: (i) to adjust the two sides of BSE in order to minimize their difference, or (ii) to adjust amplitude Γ (with choice of parameters A_i) in such a way that decay constants (supplemented by the BS normalizer) give a very good fitting to experimental results.

To find the coefficients, A_i, we calculated the difference $[\hat{q}^2(\mathrm{LHS\text{-}RHS})]$ for the determinantal form of BSE in Eq. (36) at several chosen values of $\hat{q}$, together with differences between $[f_V - f_V^{\mathrm{EXP}}]$, and then we found values of coefficients A_i that minimize those differences for all the five vector mesons studied.

Thus, we obtained a number of sets of unknown parameters A_i's. Our approach gives no unique solution, but we chose the best set of values of A_i that not only gave a reasonable agreement with the experimental f_V values, but also a good agreement between the numerical values of the LHS and RHS of the BSE in Eq. (36) as well as the agreement between the plots of their integrands for all the five vector mesons studied. Only this would ensure that the hadron-quark vertex Γ given by Eq. (29) (with unknown coefficients A_i) is indeed a solution of the BSE, though the general form of Γ has been shown to be derivable from BSE [given in details in Eqs. (17)–(29)].

Using this twin criterion we selected the best set of coefficients that should respectively be $A_0 = 1$, $A_1 = 0.0064$, $A_2 = 0.0048$, $A_3 = -0.453$, $A_4 = -0.79$, and $A_5 = -2.08474$ to predict the decay constant values $f_\rho = 0.192$ GeV, $f_\omega = 0.194$ GeV, $f_\phi = 0.220$ GeV, $f_\psi = 0.406$ GeV, and $f_Y = 0.7097$ GeV. These decay constant values have an average error with respect to the experimental data of 3.58%. Table I contains numerical values of decay constants for all the five mesons and are compared with data. Comparison of calculated decay widths $\Gamma^{\mathrm{TH.}}$ under BSE-CIA with the experimental decay widths, Γ^{EXP} is given in Table II. The plots of integrands of f_V for all the five mesons are given in Fig. 2. In Fig. 3, the amplitudes f_V for all the five studied mesons are represented on a vertical scale in units of GeV.

These coefficients A_i's selected from the twin criterion above also gave a good agreement between the numerical values of the LHS and RHS of the BSE as well as the plots of their integrands. The numerical values for the LHS and RHS along with their percentage errors for various mesons are given in Table III. The behavior of the plots of integrands for the LHS and RHS of the BSE in Eq. (36) with $\hat{q}$ for the above set of coefficients A_i is given in Fig. 4. It is seen that for ρ and ω mesons, the percentage error between numerical values of the LHS and RHS is 7.04% and 8.7%, respectively. This drops to 4.9% for the ϕ meson and is 5.84% for the Ψ meson. But for the Y meson, this disagreement is 0.27%. Thus the average error between the numerical values of the LHS and RHS of the BSE for the above set of parameters for all the five mesons is 5.34%.

However, if we do not use the determinant form of BSE in Eq. (36), and instead equate the (ij)th elements of the block diagonal 2×2 form of BSE in Eq. (34), we get four equations of which two equations corresponding to elements on main diagonal of Eq. (34) are identical. Now minimizing the difference for the elements of the LHS and RHS of this block diagonal 2×2 form of BSE in Eq. (34) means minimizing the difference for all $(\mathrm{LHS}_{ij} - \mathrm{RHS}_{ij})$ in this equation. Interestingly, we found that coefficients A_i's

TABLE II. Calculated decay widths $\Gamma^{\mathrm{TH.}}$ for the process $V \to \gamma^* \to e^+ + e^-$ (in keV) for ρ, ω, ϕ, ψ, and Y mesons in BSE-CIA along with their experimental values [25] for the set of parameters $A_0 = 1$, $A_1 = 0.0064$, $A_2 = 0.0048$, $A_3 = -0.453$, $A_4 = -0.79$, and $A_5 = -2.08474$ (giving f_V values with average error with respect to experimental data of 3.58%).

	$\Gamma^{\mathrm{TH.}}$ (keV)	Γ^{EXP} (keV)
$\rho(770)$	5.342	7.04 ± 0.06
$\omega(782)$	0.596	0.60 ± 0.02
$\phi(1020)$	1.1766	1.27 ± 0.04
$\psi(1S)(3096)$	5.281	5.5 ± 0.1
$Y(1S)(9460)$	1.320	1.312 ± 0.02

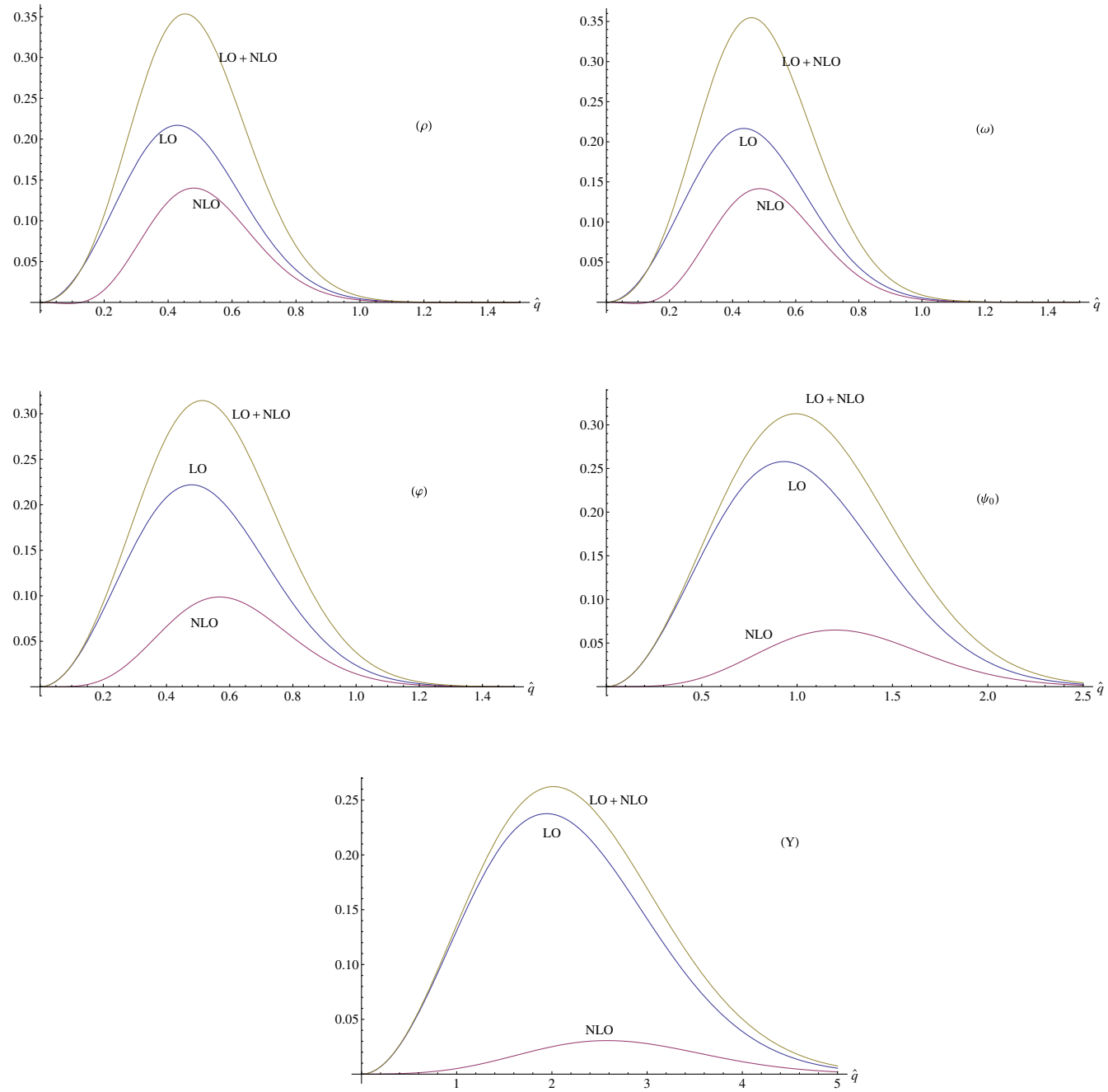

FIG. 2 (color online). Plots of integrand functions that give rise to f_V^{LO}, f_V^{NLO}, and f_V, as functions of $\hat{q}$, for the five vector mesons ρ, ω, ϕ, ψ, and Y, respectively, for the set of coefficients, $A_0 = 1, A_1 = 0.0064, A_2 = 0.0048, A_3 = -0.453, A_4 = -0.79$, and $A_5 = -2.08474$.

$(A_0 = 1, \quad A_1 = 0.0064, \quad A_2 = 0.0048, \quad A_3 = -0.453, A_4 = -0.79$, and $A_5 = -2.08474)$ obtained by minimizing Det LHS − Det RHS [as in Eq. (36)] also lead to an element-by-element minimization $(\mathrm{LHS}_{11} - \mathrm{RHS}_{11})$, $(\mathrm{LHS}_{12} - \mathrm{RHS}_{12})$, $(\mathrm{LHS}_{21} - \mathrm{RHS}_{21})$ and $(\mathrm{LHS}_{22} - \mathrm{RHS}_{22})$ in Eq. (34) for all the five mesons, ρ, ω, ϕ, ψ, and Y. We have checked this fact by drawing plots of all these differences for all the five mesons, which, in fact, have very similar forms to the plots of Fig. 4.

The normalization factors N_V were found to be $N_\rho = 0.204\ \mathrm{GeV}^{-3}$, $N_\omega = 0.199\ \mathrm{GeV}^{-3}$, $N_\phi = 0.1022\ \mathrm{GeV}^{-3}$, $N_\psi = 0.00913\ \mathrm{GeV}^{-3}$, and $N_Y = 0.00054\ \mathrm{GeV}^{-3}$. Values of f_V along with the contributions from various covariants and experimental results are listed in Table I.

We wish to mention that the decay widths of mesons are related to our decay constants f_V by formula

$$\Gamma = \frac{4\pi\alpha^2 e_Q^2 |f_V|^2}{3M}. \tag{52}$$

Here, M is the meson mass, α is the QED coupling constant (i.e., the fine structure constant), e_Q plays the

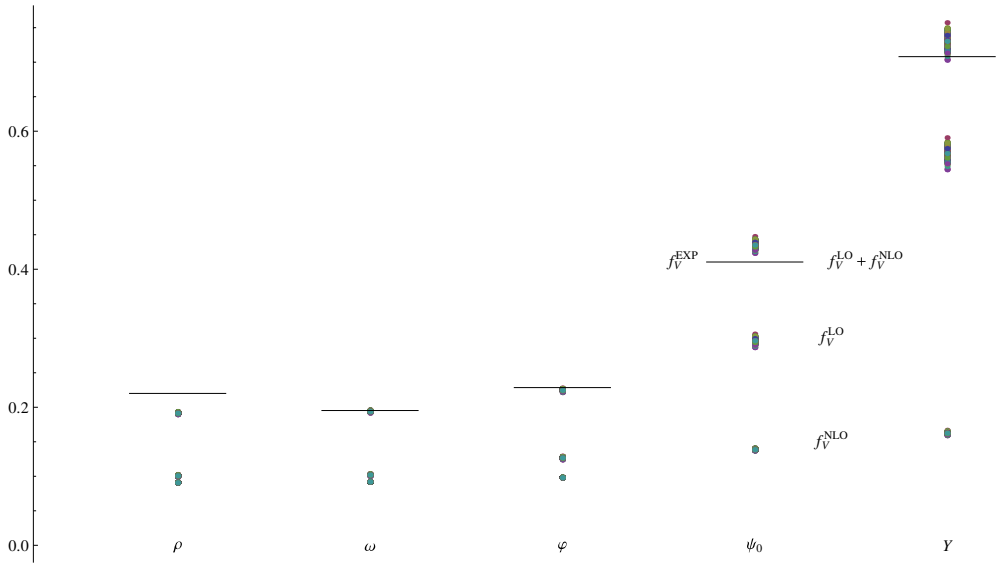

FIG. 3 (color online). Amplitudes f_V for all studied mesons are represented. Vertical scale is in units of GeV. Short horizontal lines are values obtained from experimental data. Lower sets of points are the NLO contributions obtained from our model. Intermediate sets of points are our LO results. Upper sets of points are our theoretical values of $f_V = f_V^{LO} + f_V^{NLO}$. It is concluded that the same set of A_i coefficients predicts simultaneously the f_V for all five studied mesons and that uncertainties in the A_i are strongly "amplified" for Y and ψ_0.

role of effective electric charge of the meson with values [listed after Eq. (39)] for different vector mesons. From formula (52) were obtained the data for f_V^{EXP}. A comparison of our results with those of other models and data is presented in Table IV.

B. The results

Formulas found in Sec. II express decay constants f_V of vector mesons in terms of the constant parameters A_0, A_1, A_2, A_3, A_4, A_5 as

$$f_V = \sum_{i=0}^{5} f_V^i \equiv \sum_{i=0}^{5} \frac{f_{V_i}}{N_V} A_i, \tag{53}$$

where the expression for normalizer (50) has the form

$$\frac{1}{N_V^2} = \sum_{i=0}^{5} \sum_{j=i}^{5} I_{ij} A_i A_j, \tag{54}$$

with matrix elements I_{ij} given in Eq. (A2). It can thus be seen that the expression for f_V in Eq. (51) due to the presence of BS normalizer N_V is a highly nonlinear function of the A_i's (for $i = 0, 1, 2, 3, 4, 5$). Analytical expressions for the A_i's as functions of quark masses and other parameters corresponding to each of the vector mesons cannot be obtained. However, numerical methods mentioned above give acceptable solutions of the problem.

With the parameters A_i we worked out using the procedure of calculating the difference $\hat{q}^2$[LHS–RHS] of BSE in Eq. (36) at several chosen values of $\hat{q}$, together with differences between $[f_V - f_V^{EXP}]$, and then finding values of coefficients A_i that minimize those differences, our model should be capable of predicting the values of the decay constants for the ρ, ω, ϕ, ψ, ψ', and Y mesons. We made different checks and selected the parameter set giving the results shown in Table I, which predicts the decay constants f_V's for all the five mesons that match approximately with data.

This set of parameters $A_0 = 1$, $A_1 = 0.0064$, $A_2 = 0.0048$, $A_3 = -0.4530$, $A_4 = -0.7900$, and $A_5 = -2.0847$ is also responsible for the simultaneous matching of numerical values of LHS and RHS of the BSE in Eq. (36), as well as the plots of their integrands at all values of $\hat{q}$, and thus they are to a good approximation also the solutions of BSE as well. The results of this matching of the LHS and RHS is presented in Table III, which shows the numerical values of the LHS and RHS and the errors between them from the ρ to Y meson. It is seen that for ρ and ω mesons, the percentage error between numerical values of the LHS and RHS is 7.04% and 8.73%, respectively. This drops to 4.9% for the ϕ meson and is 5.84% for the Ψ meson. But for the Y meson, this disagreement is 0.27%. Thus the average error between the numerical values of the LHS and RHS of the BSE for the above set of parameters for all the five mesons is 5.34%.

TABLE III. Numerical values of the LHS and RHS of BSE [in Eq. (34)], along with the percentage error for the five mesons for the set of parameters $A_0 = 1$, $A_1 = 0.0064$, $A_2 = 0.0048$, $A_3 = -0.453$, $A_4 = -0.79$, and $A_5 = -2.08474$.

	LHS	RHS	% Error
$\rho(770)$	0.1608	0.1730	7.04%
$\omega(782)$	0.1758	0.1926	8.73%
$\phi(1020)$	1.156	1.216	4.9%
$\psi(1S)$	1.210×10^3	1.285×10^3	5.84%
Y	4.089×10^6	4.078×10^6	0.277%

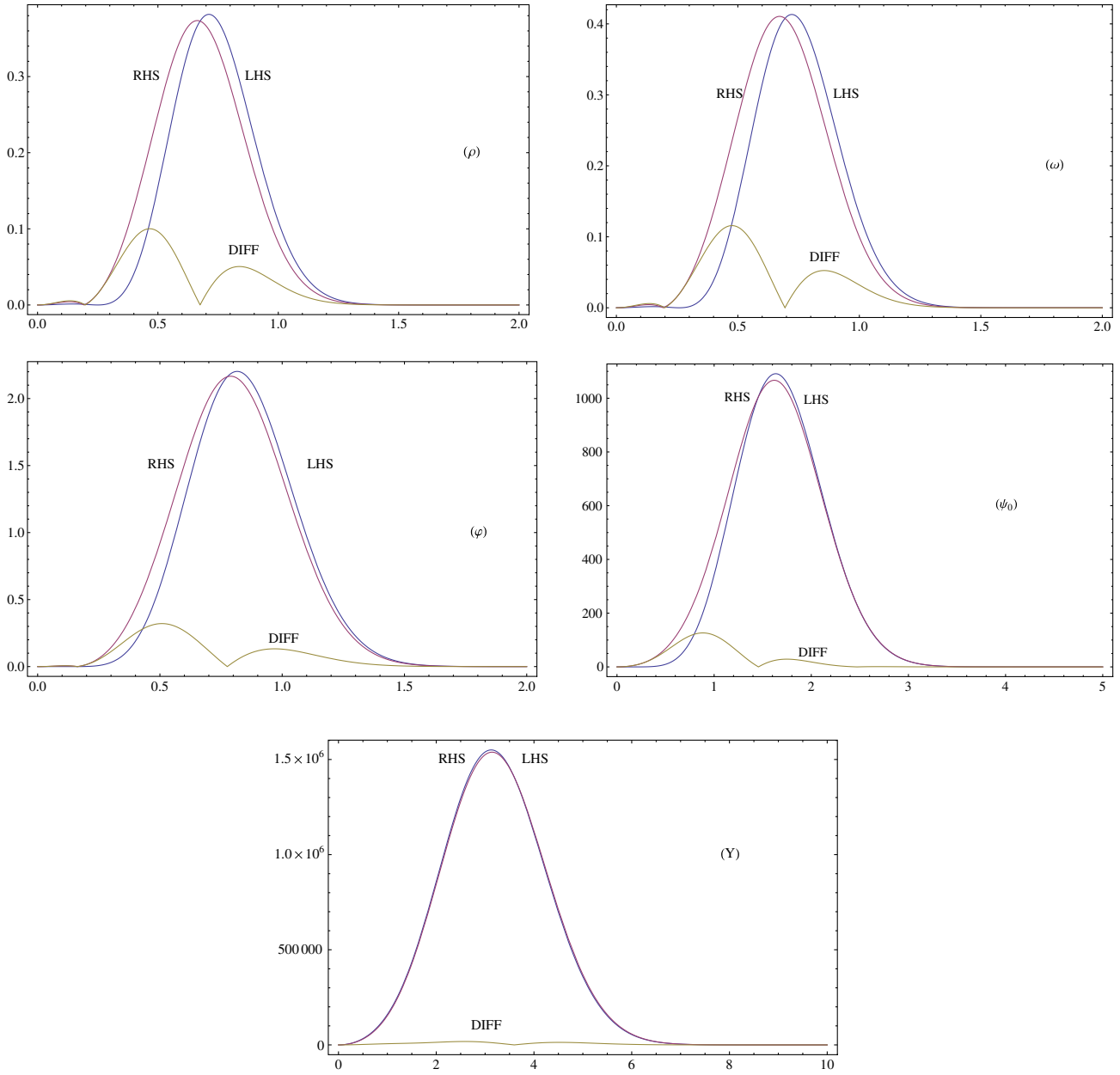

FIG. 4 (color online). Plots of integrand functions of the LHS and RHS of BSE and the absolute value of their difference (DIFF) as functions of $\hat{q}$, for the five vector mesons ρ, ω, ϕ, ψ, and Y, respectively, for the set of coefficients $A_0 = 1$, $A_1 = 0.0064$, $A_2 = 0.0048$, $A_3 = -0.453$, $A_4 = -0.79$, and $A_5 = -2.08474$.

Similarly if one notices the plots of the integrands of the LHS and RHS (vs $\hat{q}$) of the BSE in Eq. (36), one can notice the complete similarity of patterns for all the five mesons. And this trend in numerical values mentioned above is also displayed by these plots, and their difference (DIFF) as a function of ($\hat{q}$) for the five mesons.

V. DISCUSSION

In this paper we have calculated the decay constants f_V of vector mesons ρ, ω, ϕ, ψ, and Y in BSE under CIA using the hadron-quark vertex function that incorporates various Dirac covariants order by order in powers of inverse of meson mass within its structure in accordance with a recently proposed power counting rule from their complete set. This power counting rule suggests that the maximum contribution to any meson observable should come from Dirac structures associated with LO terms alone, followed by Dirac structures associated with NLO terms in the vertex function. Incorporation of all these covariants is found to bring calculated f_V values much closer to results of experimental data [25] and some recent calculations [1–8] for ρ, ω, ϕ, ψ, and Y mesons.

For calculating the coefficients A_i, we calculated the difference $\hat{q}^2$[LHS-RHS] for the BSE in Eq. (36) at several

TABLE IV. Decay constant f_V values (in GeV) for ρ, ω, ϕ, ψ, and Y mesons in BSE-CIA and their comparison with other models and data for the set of parameters, $A_0 = 1$, $A_1 = 0.0064$, $A_2 = 0.0048$, $A_3 = -0.453$, $A_4 = -0.79$, and $A_5 = -2.08474$.

	f_ρ	f_ω	f_ϕ	f_ψ	f_Y
BSE-CIA	0.192	0.194	0.220	0.406	0.7097
BSE [4]	0.215		0.224		
SDE [2]	0.163				
SDE [7]	0.207		0.259		
BSE [8]				0.459	0.498
Exp. [22]	0.2201 ± 0.0009	0.195 ± 0.003	0.228 ± 0.003	0.410 ± 0.003	0.708 ± 0.005

chosen values of $\hat{q}$, together with differences in $[f_V - f_V^{\rm EXP}]$, and then we found values of coefficients A_i that minimize those differences for all the five mesons studied. Our approach gives no unique solution, but we chose the best set of values of A_i that not only gave a reasonable agreement with the experimental f_V values, but also a good agreement between the numerical values of the LHS and RHS of the BSE in Eq. (36) as well as the agreement between the plots of their integrands, since only this would ensure that the hadron-quark vertex Γ given by Eq. (29) is indeed a solution of the BSE, though the general form of Γ (in terms of unknown parameters A_i) has been shown to be derivable from BSE [given in detail in Eqs. (17)–(29)]. This set of values of coefficients A_i is $A_0 = 1, A_1 = 0.0064, A_2 = 0.0048$, $A_3 = -0.453$, $A_4 = -0.79$, and $A_5 = -2.08474$, to predict the decay constant values, $f_\rho = 0.192$ GeV, $f_\omega = 0.194$ GeV, $f_\phi = 0.220$ GeV, $f_\psi = 0.406$ GeV, and $f_Y = 0.7097$ GeV. These decay constant values have an average error with respect to the experimental data of 3.58%.

These coefficients A_i deduced above are also the solutions of the BSE. The results of numerical values of the LHS and RHS of the BSE in Eq. (36) for all the five mesons and the percent error between them is presented in Table III, while the plots of the integrands of the LHS and RHS as a function of $\hat{q}$ for all the five mesons is presented in Fig. 4. It is seen from Table III that for ρ and ω mesons, the error between numerical values of LHS and RHS is 7.02% and 8.7%, respectively. This drops to 4.9% for the ϕ meson and is 5.84% for the Ψ meson. And for the Y meson, this error is 0.27%. Thus the average error between the numerical values of the LHS and RHS of the BSE for the above set of parameters for all the five mesons is 5.34%. The plots of integrands of the LHS and RHS of the BSE are presented in Fig. 4, which show a lot of similarity between the patterns for all values of $\hat{q}$.

All this suggests that the coefficients A_i deduced above, and hence the hadron-quark vertex function $\Gamma(\hat{q})$ in Eq. (29), are to a good approximation also the solutions of BSE, besides giving us f_V values in reasonable agreement with data.

The results for f_V values for ρ, ω, ϕ, ψ, and Y mesons with parameter set $A_0 = 1$, $A_1 = 0.0064$, $A_2 = 0.0048$, $A_3 = -0.453$, $A_4 = -0.79$, and $A_5 = -2.08474$ (giving f_V values with average error with respect to experimental data of 3.58%) are presented in Table I. A comparison with experimental data and other models is shown in Table III. The results of our f_V values for all the mesons from ρ to Y show reasonably good agreement with data.

In Fig. 2 we are plotting vs $\hat{q}$, the integrands of $f_V^{\rm LO}$, $f_V^{\rm NLO}$, and f_V for each of the studied mesons. Those plots show that the contribution to f_V from NLO covariants is smaller than the contribution from LO covariants for ρ, ω, ϕ, ψ, and Y mesons. And for ψ and Y mesons, the NLO contribution is much less in comparison than the LO contribution. We conclude from Table I that as far as the various contributions to decay constants f_V are concerned, for ρ and ω mesons, the LO terms contribute 53%, while NLO terms contribute 47%. However, as one goes to the ϕ meson, the LO contribution increases to 57%, while the NLO contribution is 43%. But as one goes to heavy ($c\bar{c}$ and $b\bar{b}$) mesons, for the ψ meson, the LO contribution is 71%, while the NLO contribution is 29%, and for the Y meson the LO contribution is 79%, while the NLO contribution reduces to 21%. Thus the drop in the contribution to decay constants from NLO covariants *vis-à-vis* LO covariants is more pronounced for heavy mesons ψ and Y. And among the two LO covariants, it can be seen that the most leading covariant $i\gamma_\mu$ contributes the maximum for all vector mesons from ρ to Y. The same trend in the behavior of decay constants is found in Fig. 3, where the decay constants f_V along with the contributions $f_V^{\rm LO}$ from LO covariants and the contributions $f_V^{\rm NLO}$ from the NLO covariants are represented on a vertical scale in units of GeV for all the five mesons. These results on decay constants f_V for vector mesons are completely in conformity with the corresponding results on decay constants f_P for pseudoscalar mesons K, D, D_S, and B done recently [14] where it was also noticed that the NLO contribution is much smaller than the LO contribution for heavier mesons like D, D_S, and B, and the most leading covariant was found to be γ_5. This is in conformity with the power counting rule according to which the leading order covariants γ_5 and $i\gamma_5(\gamma\cdot P)(1/M)$ (associated with coefficients A_0 and A_1) should contribute the maximum to decay constants followed by the next-to-leading order covariants $-i\gamma_5(\gamma\cdot q)(1/M)$ and $-\gamma_5[(\gamma\cdot P)(\gamma\cdot q) - (\gamma\cdot q)(\gamma\cdot P)](1/M^2)$ (associated with coefficients A_2 and A_3) in the BS wave function.

We observe in Fig. 2 that though the LO and NLO Dirac covariants are nearly sufficient to correctly predict amplitudes for ψ_0 and Y vector mesons, for ρ, ω, and ϕ mesons the LO and NLO Dirac covariants are not sufficient to predict accurately their amplitudes, and it might be necessary to include even higher order NNLO Dirac covariants in their hadron-quark vertex functions. This can also be seen from Fig. 3.

However, the numerical results for f_V for equal mass vector mesons, obtained in our framework with the use of leading order Dirac covariants along with the next to leading order Dirac covariants, along with a similar calculation for f_P done recently [14] for pseudoscalar mesons demonstrates the validity of our power counting rule, which also provides a practical means of incorporating various Dirac covariants in the BS wave function of a hadron. By this rule, we also get to understand the relative importance of various covariants to the calculation of meson observables. This would in turn help in obtaining a better understanding of the hadron structure.

ACKNOWLEDGMENTS

One of the authors (S. B.) is thankful to Professor Shi-Yuan Li, Shandong University, China for discussions, and to Department of Physics, Addis Ababa University for the facilities provided during the course of this work. J. M. thanks the support from Programa de Sostenibilidad 2014–2015 University of Antioquia. We thank the two unknown referees for their useful comments which helped in improving the manuscript.

APPENDIX: FORMULAS FOR THE $I_{ij}(m, M, \hat{q}, R)$ IN BS NORMALIZER

In Eq. (49) for the BS normalizer, the elements $I_{ij}(m, M, \hat{q}, R)$ depend on $S = (D_1, D_2, D_{11}, D_{12}, D_{22}, R)$, where the elements of S are the analytic results of contour integrations over the off-shell parameter $d\sigma$ in the complex σ plane, whose results are given in Eq. (A1),

$$
\begin{aligned}
D_1 &= \int \frac{M d\sigma}{\Delta_1^2 \Delta_2} \Delta_1 = 2\pi i \frac{1}{D(\hat{q})}, \\
D_2 &= \int \frac{M d\sigma}{\Delta_1^2 \Delta_2} \Delta_2 = 2\pi i \frac{2}{(2\omega)^3}, \\
D_{11} &= \int \frac{M d\sigma}{\Delta_1^2 \Delta_2} \Delta_1^2 = 2\pi i \frac{1}{2\omega}, \\
D_{12} &= \int \frac{M d\sigma}{\Delta_1^2 \Delta_2} \Delta_1 \Delta_2 = 2\pi i \frac{1}{2\omega}, \\
D_{22} &= \int \frac{M d\sigma}{\Delta_1^2 \Delta_2} \Delta_2^2 = 2\pi i \frac{2\omega^2 - M^2}{2\omega^3}, \\
R &= \int \frac{M d\sigma}{\Delta_1^2 \Delta_2} = 2\pi i \frac{M^2 - 12\omega^2}{4\omega^3 (M^2 - 4\omega^2)^2},
\end{aligned}
\tag{A1}
$$

Function $D(\hat{q})$ was defined in Eq. (5).

The I_{ij} have the following explicit form:

$$
\begin{aligned}
I_{00} &= \frac{1}{3}\left[\frac{1}{M^2}\left(1 - 12\frac{m^2}{M^2}\right) D_{11} + \frac{3}{M^2}\left(-1 + \frac{m^2}{M^2}\right) D_{12} + \frac{1}{M^2}(7m^4 - 3m^2M^2)R \right. \\
&\quad \left. + \frac{1}{M^2}\left(M^2 + \frac{13m^4}{M^2} - 5m^2\right) D_1 - \frac{13m^4 D_2}{M^4} + \frac{9m^2 D_{22}}{M^4}\right], \\
I_{11} &= \frac{2}{3}\left[-\frac{4D_{11}}{M^2} + \frac{3D_{12}}{M^2} - \frac{4D_{22}}{M^2} - \frac{8M^2 D_1}{M^2} + \frac{(8m^2 + M^2)D_2}{M^2} + 2(4m^2 + M^2)R\right], \\
I_{22} &= \frac{2}{3}\left[\frac{D_{11}}{M^2} + \frac{3D_{12}}{M^2} - \frac{4D_{22}}{M^2} - \frac{8m^2 D_1}{M^2} + \frac{(8m^2 + M^2)D_2}{M^2} + 2(4m^2 + M^2)R\right], \\
I_{33} &= \frac{1}{3}\left[\frac{D_{11}}{M^2}\left(\frac{-6m^4}{M^4} + \frac{9m^2}{M^2} - \frac{22m^3}{M^3} - \frac{55m^2}{2M^2} + 13\right)\right. \\
&\quad + \frac{D_{12}}{M^2}\left(\frac{18m^4}{M^4} - \frac{7m^2}{M^2} + \frac{70m^2}{M^2} + \frac{12m^3}{M^3} - 4\right) \\
&\quad + \frac{D_{22}}{M^2}\left(\frac{9m^4}{M^4} - \frac{67m^2}{M^2} + \frac{10m^3}{M^3} + 35 - \frac{9m^2}{M^2}\right) \\
&\quad + \frac{D_1}{M^2}\left(\frac{29}{2}M^2 - 13m^2 + \frac{12m^4}{M^2} - \frac{3m^3}{M} - \frac{48m^4}{M^2} + \frac{16m^6}{M^4} - \frac{36m^5}{M^3}\right) \\
&\quad + \frac{D_2}{M^2}\left(22M^2 - 7m^2 - \frac{12m^4}{M^2} + \frac{3m^3}{M} + \frac{48m^4}{M^2} - \frac{16m^6}{M^4} + \frac{4m^5}{M^3}\right) \\
&\quad \left. + \frac{R}{M^2}\left(-m^2M^2 - 14m^3M + 76m^4 + 16mM^3 + 6M^4 + \frac{5}{2}m^4\right)\right],
\end{aligned}
$$

$$
\begin{aligned}
I_{44} &= \frac{1}{3}\left[\frac{D_{11}}{M^2}\left(\frac{4m^2}{M^2}+1\right)+\frac{7D_{12}}{2M^2}+\frac{D_{22}}{M^2}\left(\frac{1}{6}-\frac{4m^2}{M^2}\right)\right.\\
&\quad+\left(2-\frac{6m^4}{M^4}-\frac{m^5}{M^5}-\frac{6m^2}{M^2}-\frac{m^3}{M^3}\right)D_1+\left(\frac{1}{6}+\frac{m^5}{M^5}+\frac{6m^4}{M^4}-\frac{8m^2}{M^2}\right)D_2\\
&\quad\left.+\left(-4m^2+\frac{8m^4}{M^2}+\frac{m^5}{M^3}+\frac{M^2}{3}\right)R\right],\\
I_{55} &= \frac{1}{3}\left[-\frac{3}{2M^2}\left(\frac{m^4}{3M^4}+\frac{11m^2}{3M^2}+\frac{3}{2}\right)D_{12}+\frac{D_1}{M^2}\left(-M^2+\frac{3m^4}{2M^2}+\frac{7m^5}{2M^3}+\frac{17m^2}{4}\right)\right.\\
&\quad\left.+\frac{D_2}{M^2}\left(-\frac{M^2}{4}-\frac{3m^5}{2M^3}-\frac{7m^4}{2M^2}+\frac{15m^2}{4}\right)+\frac{R}{M^2}\left(-\frac{3M^4}{2}+\frac{9m^2M^2}{4}+\frac{7m^4}{2}\right)R\right],\\
I_{01} &= \left[-\frac{4mD_{11}}{M^3}-\frac{8mD_{22}}{M^3}+\frac{4mD_{12}}{M^3}-\frac{4D_1}{3M}\left(\frac{4m^3}{M^2}+m\right)\right.\\
&\quad\left.+\frac{4D_2}{M}\left(\frac{4m^3}{3M^2}-m\right)+\left(\frac{16m^3}{3M}-\frac{4mM}{3}R\right)\right],\\
I_{02} &= \left[\frac{8m}{M}(D_1-D_2)-8mMR\right];\\
I_{03} &= \left[-\frac{2m}{M^3}D_{11}+\frac{4m}{3M^3}D_{12}+\frac{2m}{M^3}D_{22}+\frac{8D_1}{3M}\left(\frac{m^3}{M^2}-m\right)+\frac{3m^3}{3M^3}D_2\right.\\
&\quad\left.+\left(\frac{8m^3}{3M}-\frac{2mM}{3}\right)R\right],\\
I_{04} &= \left[-\frac{7m^2D_{11}}{3M^4}+\frac{D_{22}}{3M^2}\left(-\frac{2m^4}{M^4}-\frac{7m^2}{M^2}+8\right)+\frac{D_{12}}{3M^2}\left(\frac{2m^2}{M^2}-8\right)\right.\\
&\quad\left.+\frac{D_1}{M^2}\left(-M^2-\frac{2m^4}{3M^2}+\frac{8m^2}{3}\right)+\frac{D_2}{M^2}\left(\frac{4M^2}{3}+\frac{2m^4}{3M^2}-\frac{8m^2}{3}\right)+\frac{R}{M^2}(-m^2M^2-2m^4)\right],\\
I_{05} &= \left[\frac{D_{11}}{M^2}\left(\frac{6m^2}{M^2}-\frac{34}{3}\right)+\frac{D_{22}}{3M^2}\left(\frac{26m^2}{M^2}-14\right)-\frac{D_{12}}{3M^2}\left(\frac{44m^2}{M^2}+20\right)\right.\\
&\quad+\frac{D_1}{M^2}\left(-6M^2+\frac{8m^4}{3M^2}-12m^2\right)D_1+\frac{D_2}{M^2}\left(-\frac{22M^2}{3}-\frac{8m^4}{M^2}+\frac{44m^2}{3}\right)\\
&\quad\left.+\frac{R}{M^2}\left(14m^2M^2-\frac{8m^4}{3}-\frac{10M^4}{3}\right)\right],\\
I_{12} &= \left[\frac{D_{11}}{M^2}\left(\frac{m^2}{M^2}+\frac{2}{3}\right)+\frac{D_{22}}{M^2}\left(\frac{m^2}{M^2}-4\right)+\frac{D_{12}}{M^2}\left(-\frac{2m^2}{M^2}+\frac{10}{3}\right)\right.\\
&\quad\left.+\frac{D_1}{M^2}\left(\frac{8M^2}{3}-\frac{2m^2}{3}\right)+\frac{D_2}{M^2}\left(-2M^2+\frac{2m^2}{3}\right)+\frac{5m^2R}{3}\right],\\
I_{13} &= \left[\frac{D_{11}}{3M^3}\left(-\frac{4m^3}{M^2}-34m\right)+\frac{D_{22}}{3M^3}\left(-\frac{4m^3}{M^2}-26m\right)+\left(\frac{8m^2}{M^4}+\frac{20}{M^2}\right)D_{12}\right.\\
&\quad+\frac{D_{22}}{M^3}\left(-\frac{16m^5}{3M^4}+\frac{8m^3}{3M^2}+28m\right)+\frac{D_2}{M}\left(\frac{16m^5}{3M^4}-\frac{8m^3}{3M^2}-\frac{46m}{3}\right)\\
&\quad\left.+\left(-\frac{28m^4}{3M^2}-\frac{8m^3}{3M}-2mM\right)R\right],
\end{aligned}
$$

$$
\begin{aligned}
I_{14} &= \left[\frac{D_{11}}{M^2}\left(-\frac{m^4}{M^4}+\frac{4}{3}\right)+\frac{D_{22}}{M^2}\left(-\frac{m^2}{M^2}+2\right)+\frac{D_{12}}{M^2}\left(\frac{2m^2}{M^2}-\frac{10}{3}\right)\right.\\
&\quad\left.+\frac{D_1}{M^2}\frac{13m^2}{3}-\frac{D_2}{M^2}\frac{5m^2}{3}+\left(-\frac{8m^2}{3}+\frac{2M^2}{3}\right)R\right],\\
I_{15} &= \left[\frac{5m}{3M^3}D_{11}-\frac{m}{3M^3}D_{22}-\frac{4m}{3M^3}D_{12}+\frac{D_2}{M}\left(-\frac{2m^3}{M^2}+\frac{2m}{3}\right)D_2+\left(-\frac{2m^3}{M}+mM\right)R\right],\\
I_{23} &= \left[\left(\frac{7m^3}{3M^5}+\frac{3m^2}{4M^4}+\frac{5m}{12M^3}\right)D_{11}+\left(\frac{7m^3}{3M^5}-\frac{3m^2}{6M^4}\right)D_{22}\right.\\
&\quad+\left(-\frac{14m^3}{3M^5}+\frac{m}{3M^3}-\frac{3m^2}{4M^4}\right)D_{12}\\
&\quad+\left(-\frac{7m^3}{6M^3}+\frac{m}{6M}-\frac{3m^4}{8M^4}+\frac{3m^2}{8M^2}\right)D_1+D_2\left(\frac{7m^3}{6M^3}-\frac{m}{M}+\frac{3m^4}{8M^4}\right)\\
&\quad\left.+\left(\frac{5m^3}{6M}-\frac{mM}{4}+\frac{3m^4}{16M^2}\right)R\right];\\
I_{24} &= \left[\frac{13m^3}{M}R+\frac{D_{11}}{M^3}\left(-\frac{3m^3}{2M^2}+\frac{7m}{3}\right)-\frac{D_{22}}{M^3}\left(\frac{m^3}{3M^2}+6m\right)+\frac{D_{12}}{M^3}\left(\frac{3m^3}{M^2}+\frac{11m}{3}\right)\right.\\
&\quad\left.+\frac{D_1}{3M}\left(-\frac{25m^3}{M^2}-5m\right)+\frac{D_2}{3M}\left(\frac{25m^3}{M^2}-19m\right)\right],\\
I_{25} &= \left[\frac{D_{11}}{M^2}\left(-\frac{3m^2}{2M^2}+\frac{4m^4}{M^4}+1\right)+\frac{D_{22}}{M^2}\left(-\frac{7m^2}{2M^2}-\frac{4m^4}{3M^4}+\frac{10}{3}\right)\right.\\
&\quad+\frac{D_1}{M^2}\left(\frac{7M^2}{6}+\frac{m^4}{M^2}-10\frac{4m^2}{3}-\frac{8m^6}{3M^4}\right)+\frac{D_2}{M^2}\left(\frac{8M^2}{3}-\frac{m^4}{3M^2}+\frac{8m^6}{3M^4}-8m^2\right)\\
&\quad\left.+\frac{D_1D_2}{M^2}\left(\frac{5m^2}{M^2}-\frac{8m^4}{3M^4}+2\right)+\left(-\frac{23m^2}{6}+\frac{19m^4}{3M^2}+\frac{8m^6}{3M^4}+\frac{2M^2}{3}\right)R\right],\\
I_{34} &= \left[-\frac{m^3}{M^5}(D_{11}+D_{22})+\frac{4m^3}{M^5}D_{12}\right],\\
I_{35} &= \left[\frac{D_{11}}{M^2}\left(\frac{m^4}{M^4}+\frac{28m^2}{M^2}-\frac{16m^4}{M^4}-\frac{14}{3}\right)+\frac{D_{22}}{M^2}\left(\frac{m^2}{M^2}-\frac{8m^4}{3M^4}+\frac{16m^3}{M^3}-\frac{2}{3}\right)\right.\\
&\quad+\frac{D_1}{M^2}\left(\frac{2M^2}{3}-\frac{10m^3}{M}-\frac{2m^4}{3M^2}+\frac{16m^6}{3M^4}+\frac{22m^2}{3}\right)+\frac{D_2}{M^2}\left(2M^2-\frac{12m^2}{3}+\frac{26m^4}{3M^2}-\frac{2m^4}{3M^2}-\frac{16m^6}{3M^4}\right)\\
&\quad\left.+\frac{D_{12}}{M^2}\left(-\frac{2m^4}{3M^4}+\frac{50m^2}{3M^2}+\frac{4}{3}\right)+\frac{R}{M^2}\left(-2m^4-\frac{8M^4}{3}-\frac{14m^6}{3M^2}-\frac{10m^2M^2}{3}\right)\right],\\
I_{45} &= \left[\frac{D_{11}}{M^3}\left(-\frac{8m^3}{M^2}-\frac{8m}{3}\right)+\frac{D_{22}}{M^3}\left(-\frac{8m^3}{M^2}+\frac{16m}{3}\right)+\frac{D_{12}}{M^3}\left(\frac{16m^3}{M^2}-\frac{8m}{3}\right)\right.\\
&\quad\left.\frac{D_1}{M^2}\left(\frac{8m^3}{M^2}-\frac{4m}{3}\right)+\frac{D_2}{M}\left(-\frac{8m^3}{M^2}+\frac{4m}{3}\right)\right].
\end{aligned}
\tag{A2}
$$

[1] R. Alkofer, P. Watson, and H. Weigel, Phys. Rev. D **65**, 094026 (2002).

[2] M. A. Ivanov, Yu. A. Kalinovski, and C. D. Roberts, Phys. Rev. D **60**, 034018 (1999).

[3] F. E. Close, A. Donnachi, and Yu. S. Kalashnikova, Phys. Rev. D **65**, 092003 (2002).

[4] H.-M. Li and S.-L. Wan, Chin. Phys. Lett. **25**, 1239 (2008).

[5] G. Cvetič, C. S. Kim, G.-Li Wang, and W. Namgung, Phys. Lett. B **596**, 84 (2004).
[6] D. S. Hwang and G. H. Kim, Phys. Rev. D **55**, 6944 (1997).
[7] R. Alkofer and L. W. Smekel, Phys. Rep. **353**, 281 (2001).
[8] G. L. Wang, Int. J. Mod. Phys. A **23**, 3263 (2008).
[9] A. N. Mitra and B. M. Sodermark, Nucl. Phys. **A695**, 328 (2001), and references therein.
[10] A. N. Mitra, Proc. Indian Natl. Sci. Acad. **65**, 527 (1999).
[11] S. Bhatnagar, D. S. Kulshreshtha, and A. N. Mitra, Phys. Lett. B **263**, 485 (1991).
[12] A. N. Mitra and S. Bhatnagar, Int. J. Mod. Phys. A **07**, 121 (1992).
[13] S. Bhatnagar and S.-Y. Li, J. Phys. G **32**, 949 (2006).
[14] S. Bhatnagar, S.-Y. Li, and J. Mahecha, Int. J. Mod. Phys. E **20**, 1437 (2011).
[15] C. H. L. Smith, Ann. Phys. (N.Y.) **53**, 521 (1969).
[16] F. T. Hawes and M. A. Pichowsky, Phys. Rev. C **59**, 1743 (1999).
[17] E. Mengesha and S. Bhatnagar, Int. J. Mod. Phys. E **20**, 2521 (2011).
[18] H. Sazdjian, J. Math. Phys. (N.Y.) **28**, 2618 (1987).
[19] S. Chakravorty, K. K. Gupta, N. N. Singh, and A. N. Mitra, Prog. Part. Nucl. Phys. **22**, 43 (1989).
[20] J. S. Goldstein, Phys. Rev. **91**, 1516 (1953).
[21] S. Bhatnagar, Int. J. Mod. Phys. E **14**, 909 (2005).
[22] K. K. Gupta, A. N. Mitra, and N. N. Singh, Phys. Rev. D **42**, 1604 (1990).
[23] D. Arndt and C.-R. Ji, Phys. Rev. D **60**, 094020 (1999).
[24] S. Bhatnagar and S. Y. Li, in *Proceedings of 9th Workshop on Non-Perturbative Quantum Chromodynamics, Paris, France, 2007*, pp 12, www.slac.stanford.edu/econf/c0706044/pdf/12.pdf.
[25] J. Beringen *et al.* (Particle Data Group), Phys. Rev. D **86**, 010001 (2012).